Journal of Medicinal Chemistry

Article

Synthesis and Structure–Activity Relationships of Pyrazine-Pyridine Biheteroaryls as Novel, Potent, and Selective Vascular Endothelial Growth Factor Receptor-2 Inhibitors

Gee-Hong Kuo, Catherine Prouty, Aihua Wang, Stuart Emanuel, Alan DeAngelis, Yan Zhang, Fengbin Song, Lawrence Beall, Peter J. Connolly, Prahba Karnachi, Xin Chen, Robert H. Gruninger, Jan Sechler, Angel Fuentes-Pesquera, Steven A. Middleton, Linda Jolliffe, and William V. Murray

J. Med. Chem., **2005**, 48 (15), 4892-4909• DOI: 10.1021/jm058205b • Publication Date (Web): 24 June 2005

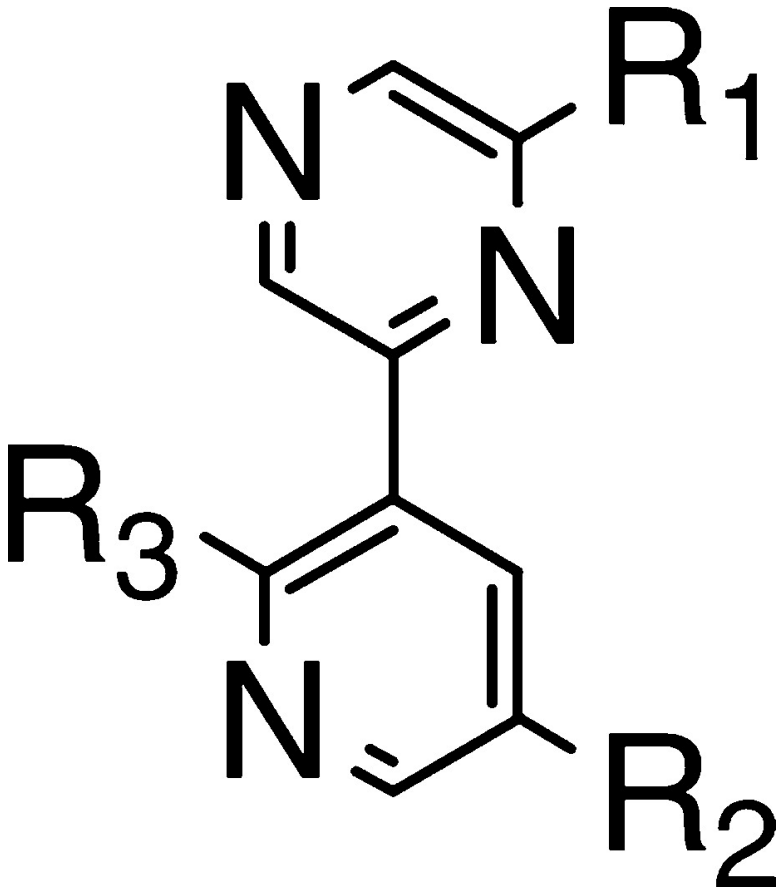

Synthesis and Structure−Activity Relationships of Pyrazine-Pyridine Biheteroaryls as Novel, Potent, and Selective Vascular Endothelial Growth Factor Receptor-2 Inhibitors

Gee-Hong Kuo,* Catherine Prouty, Aihua Wang, Stuart Emanuel, Alan DeAngelis, Yan Zhang, Fengbin Song, Lawrence Beall, Peter J. Connolly, Prahba Karnachi, Xin Chen, Robert H. Gruninger, Jan Sechler, Angel Fuentes-Pesquera, Steven A. Middleton, Linda Jolliffe, and William V. Murray

Drug Discovery Division, Johnson & Johnson Pharmaceutical Research and Development, L.L.C., 1000 Route 202, P.O. Box 300, Raritan, New Jersey 08869

Received March 4, 2005

There is much evidence that direct inhibition of the kinase activity of vascular endothelial growth factor receptor-2 (VEGFR-2) will result in the reduction of angiogenesis and the suppression of tumor growth. Palladium-catalyzed C−C bond, C−N bond formation reactions were used to assemble various pyrazine-pyridine biheteroaryls as potent VEGFR-2 inhibitors. Among them, 4-{5-[6-(3-chloro-phenylamino)-pyrazin-2-yl]-pyridin-3-ylamino}-butan-1-ol (**39**) and *N*-{5-[6-(3-chloro-phenylamino)-pyrazin-2-yl]-pyridin-3-yl}-*N*′,*N*′-dimethyl-ethane-1,2-diamine (**41**) exhibited the highest kinase selectivity against fibroblast growth factor receptor kinase, platelet-derived growth factor receptor kinase, and glycogen synthase kinase-3. All of these compounds showed good cellular potency to inhibit VEGF-stimulated proliferation of human umbilical vein endothelial cells (HUVEC) but with modest effects on the unstimulated growth of HUVEC. The low inhibition of these compounds to the growth of tumor cell lines, such as HeLa, HCT-116, and A375 further confirms that these VEGFR-2 inhibitors are not cytotoxic agents. The in vivo antitumor activity of **39** and **41** were demonstrated in the A375 human melanoma xenograft nude mice model. Molecular modeling (QSAR analysis) was conducted in an attempt to rationalize the observed structure−activity relationship.

Introduction

Angiogenesis, the formation of new capillaries from preexisting blood vessels,[1] is a necessary process for organ development during embryogenesis and is critical for the female reproductive cycle, inflammation, and wound healing in the adult.[2] Pathological angiogenesis is associated with disease states such as cancer,[3] diabetic retinopathy,[4] rheumatoid arthritis,[5] endometriosis,[6] and psoriasis.[7] Solid tumors, in particular, are dependent on angiogenesis to grow beyond a certain critical size by inducing new capillaries sprouting from existing blood vessels to secure their nutrition, oxygen supply, and waste removal.[3,8] In addition, angiogenesis also promotes metastasis of tumor cells to other sites.[9]

The new vessel growth and maturation are highly complex and coordinated processes, requiring the stimulation by a number of growth factors,[10] but vascular endothelial growth factor (VEGF) signaling often represents a critical rate-limiting step in physiological angiogenesis and pathological angiogenesis.[11] The biological effects of VEGF are mediated by two receptor tyrosine kinases (RTKs), VEGFR-1 (Flt-1)[12] and VEGFR-2 [also known as kinase domain region (KDR) or Flk-1].[13] While the precise function of VEGFR-1 is still under debate,[14] there is much evidence that VEGFR-2 is the major mediator of vascular endothelial cell (EC) mitogenesis and survival, as well as angiogenesis and microvascular permeability.[14] Therefore, it is expected that direct inhibition of the kinase activity of VEGFR-2 will result in the reduction of angiogenesis and the suppression of tumor growth. Furthermore, inhibition of VEGFR-2 targeting the genetically more stable host ECs instead of labile tumor tissues may decrease the chance of resistance development.[15]

A number of VEGF inhibitors are currently undergoing clinical trials in advanced stage for the treatment of cancer, including a humanized monoclonal antibody to VEGF (bevacizumab/rhuMab VEGF),[16] an anti-VEGFR-2 antibody,[17] a soluble VEGF receptor,[18] and several small-molecule VEGFR-2 inhibitors (PTK787/vatalanib **80**,[19] SU-11248 **81**,[20] SU-6668 **82**,[21] and ZD-6474 **83**,[22] Scheme 1). Among them, bevacizumab in combination with chemotherapy[16,23] was accepted by FDA in 2003 for the treatment of first-line metastatic colorectal cancer. This first proof-of-concept example will certainly warrant the development of many more small-molecule VEGF inhibitors[24] for anti-angiogenesis therapy.

In an attempt to identify a potent and selective cyclin-dependent kinase-1 (CDK1) inhibitor, we unexpectedly discovered a pyrazine-pyridine scaffold, with 1,3-substitution-orientation at both upper and lower rings (Scheme 1, Targets I), exhibiting high inhibitory potency at VEGFR-2.[25] This article describes our continued efforts in the structure−activity relationships (SAR) studies and toward the identification of pyrazine-pyridine biheteroaryls as potent and selective VEGFR-2 inhibitors. The in vivo antitumor activity in mice model was also demonstrated.

* To whom correspondence should be addressed. Tel: 908-704-4330. Fax: 908-203-8109. E-mail: gkuo@prdus.jnj.com.

10.1021/jm058205b CCC: $30.25
Published on Web 06/24/2005

Scheme 1

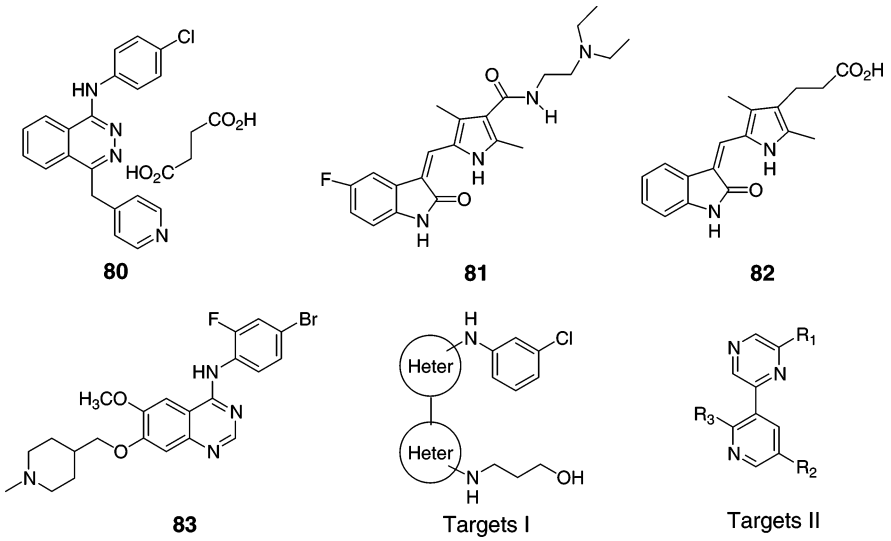

Scheme 2[a]

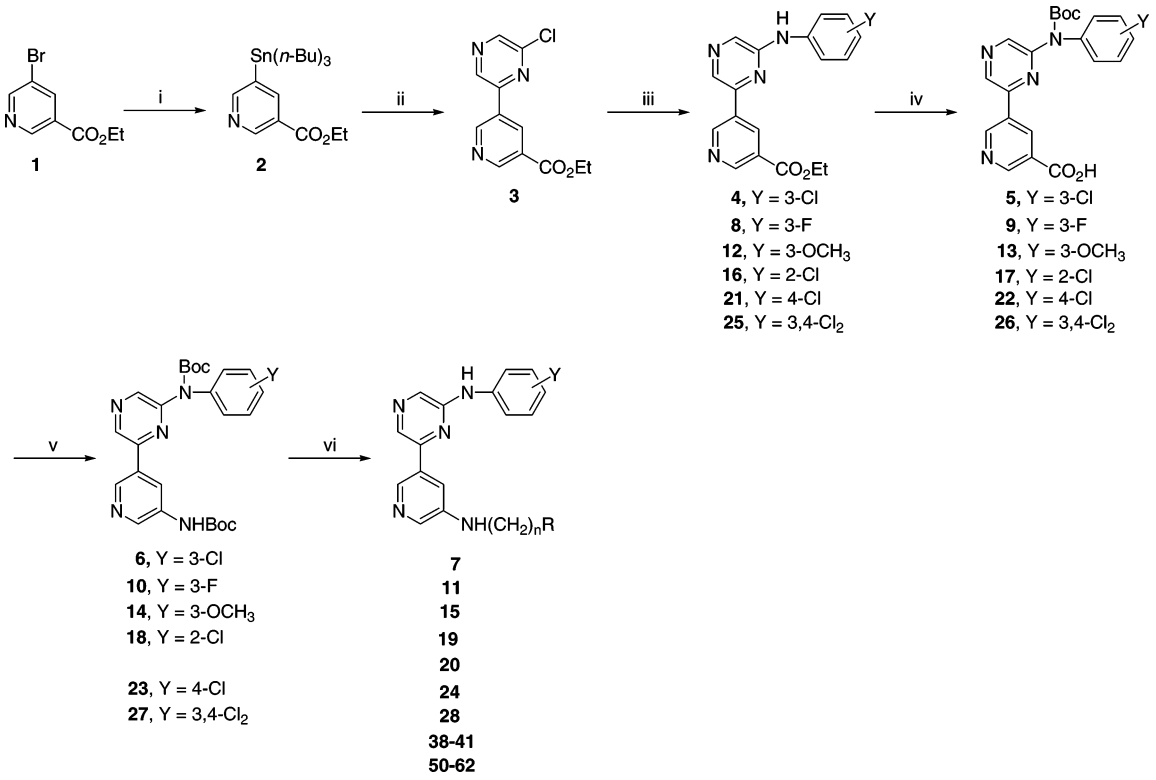

[a] (i) $[(n\text{-}Bu)_3Sn]_2$, $Pd(OAc)_2$, P(*o*-Tol)$_3$, 100 °C; (ii) 2,6-dichloropyrazine, $Pd(PPh_3)_2Cl_2$, LiCl, 100 °C; (iii) substituted aniline, $Pd_2(dba)_3$, DPPF, Cs_2CO_3, 110 °C; (iv) (a) Boc_2O, DMAP, (b) NaOH, 0−20 °C; (v) DPPA, Et_3N, *t*-BuOH, 65−100 °C; (vi) (a) $X(CH_2)_nR^1$, Cs_2CO_3, 70 °C, (b) TFA.

Chemistry

The 3,3′-disubstituted pyrazine-pyridine targets II (Scheme 1) were assembled based upon three key steps: (1) a palladium-catalyzed Stille reaction[26] to form the C−C bond that connected the pyrazine ring and pyridine ring, (2) a palladium-catalyzed cross-coupling reaction to form the C−N bond[27a] or C−O bond[27b] that installed the substituent on the pyrazine ring, (3) a Curtius rearrangement[28] to form the C−N bond that introduced the substituent on the pyridine ring.

For example, a Stille coupling reaction of organo-stannane **2** with 2,6-dichloropyrazine catalyzed by $Pd(PPh_3)_2Cl_2$[29] gave **3** (Scheme 2). The organo-stannane **2** was prepared by the palladium-catalyzed transformation from the organo-bromide **1**.[30] The palladium-catalyzed amination reaction of **3** with 3-chloroaniline in the presence of DPPF[31] as the ligand generated **4**. Boc-protection, base hydrolysis, followed by Curtius rearrangement provided **6.** Alkylation of **6** with (3-bromopropoxy)-*t*-butyl-dimethylsilane, followed by TFA deprotection, gave the first target molecule **7** (Scheme 2, Table 1). Replacing 3-chloroaniline with 3-fluoro-aniline (3-methoxyaniline or 2-chloroaniline), following the same procedure as in the preparation of **7** gave **11**

Table 1. Binding Affinities at CDK1 and VEGFR-2[a]

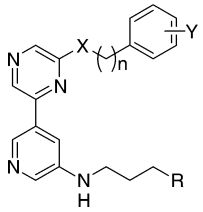

					$IC_{50} \pm SEM$[b] (μM)	
compd	X	N	Y	R	CDK1	VEGFR-2
7	NH	0	3-Cl	OH	>10	0.084 ± 0.014
11	NH	0	3-F	OH	>10	0.168 ± 0.002
15	NH	0	3-OCH_3	OH	>10	0.740 ± 0.070
19	NH	0	2-Cl	OH	>10	1.010 ± 0.300
20	NH	0	3-Cl	4-pyridine	>10	0.076 ± 0.024
24	NH	0	4-Cl	4-pyridine	>10	1.0 ± 0.2
28	NH	0	3,4-Cl_2	4-pyridine	>10	0.189 ± 0.080
32	NH	1	H	OH	>10	1.05 ± 0.18
36	O	0	3-Cl	OH	>10	>10

[a] Assay details were described in Experimental Section. [b] SEM: standard error mean.

(**15** or **19**). On the other hand, alkylation of **6** with 4-(3-chloropropyl)pyridine followed by TFA deprotection gave target molecule **20** (Scheme 2, Table 1). The pyridine analogues, **24** and **28**, were both prepared in the similar way as that of **20**. Meanwhile, alkylation of **6** with diverse halides, followed by TFA deprotection, provided target molecules **38**−**41** and **50**−**62** (Scheme 2, Table 2).

The palladium-catalyzed amination of **3** with benzylamine was conducted using the same reaction conditions as with substituted anilines to give **29** in 28% yield (Scheme 3). Boc-protection, base hydrolysis, followed by Curtius rearrangement, alkylation, and deprotection gave the target molecule **32** (Scheme 3, Table 1). Under the same palladium-catalyzed reaction conditions, C−O bond formation between **3** and 3-chlorophenol was accomplished to give **33** in modest yield (27%). Following the same reaction sequence as for the preparation of **32**, diaryl-ether analogue **36** was obtained (Scheme 3, Table 1).

The syntheses of amide and reversed-amide series were shown in Scheme 4. HATU-promoted amide bond formation of **5** with various amines gave **42** and **43** (Scheme 4, Table 2). Alkylation of **6** with substituted acetyl chlorides followed by TFA deprotection generated target molecules **44**−**49** (Scheme 4, Table 2).

The synthesis of the fluoro-pyridine **70** was shown in Scheme 5. Bromination followed by Curtius rearrangement of pyridine **63** gave **64**. Alkylation of **64** gave **65**, and reaction of **65** with $NOBF_4$ gave 3-bromo-2-fluoropyridine **66** in 62% yield. Converting the bromide **66** to the organo-stannane **67** followed by Stille coupling of **67** with **68** afforded **69**. Removal of the Cbz-, Boc-, and TBDPS-protecting groups of **69** gave the fluoro-pyridine **70**. The synthesis of the chloro-pyridine **76** was shown in Scheme 6. Bromination of **71** followed by reaction with $POCl_3$ gave **72**. Curtius rearrangement of **72** gave **73**; alkylation of **73** followed by palladium-catalyzed transformation gave organo-stannane **75**. Stille coupling of **75** with **68** gave the target molecule **76**. The aminopyridine **79** was prepared with a method similar to that of **70** as shown in Scheme 5.

Table 2. Binding Affinities at CDK1 and VEGFR-2[a]

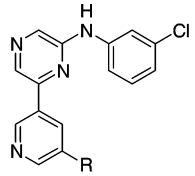

		$IC_{50} \pm SEM$ (μM)	
Compd	R	CDK1	VEGFR-2
37	NH_2	>10	1.16 ± 0.39
7	$NH(CH_2)_3OH$	>10	0.084 ± 0.014
38	$NH(CH_2)_2OH$	>10	0.275 ± 0.125
39	$NH(CH_2)_4OH$	>10	0.063 ± 0.015
40	$NH(CH_2)_3N(CH_3)_2$	>10	0.135 ± 0.045
41	$NH(CH_2)_2N(CH_3)_2$	>10	0.105 ± 0.035
42	$CONH(CH_2)_2N(CH_3)_2$	3.69	4.3 ± 1.4
43	$CONH(CH_2)_3OH$	>10	2.38 ± 0.12
44	$NHCOCH_2OH$	>10	0.346 ± 0.064
45	$NHCOCH_2OCH_3$	>10	0.303 ± 0.047
46	$NHCO(CH_2)_2OCH_3$	>10	0.593 ± 0.003
47	$NHCOCH_2OCH_2Ph$	>10	>10
48	$NHCOCH_2OPh$	>10	>10
49	NHCO(4-$N(CH_3)_2$Ph)	>10	>10
50	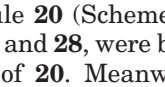	5.615 ± 1.185	0.236 ± 0.064
51	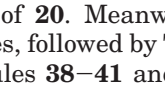	>10	0.123 ± 0.012
52	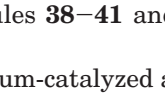	>10	0.18 ± 0.00
53	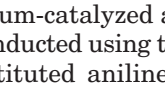	5.385 ± 0.715	0.399 ± 0.029
54	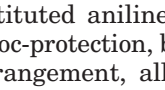	>10	0.391 ± 0.084
55	$NH(CH_2)_4$(4-pyridine)	10	0.266 ± 0.029
20	$NH(CH_2)_3$(4-pyridine)	>10	0.076 ± 0.024
56	$NH(CH_2)_3$(3-pyridine)	>10	0.076 ± 0.014
57	$NH(CH_2)_3$(1-pyrazole)	>10	0.094 ± 0.015
58	$NH(CH_2)_3$(1,2,4-triazole)	>10	0.067 ± 0.015
59	$NH(CH_2)_3Ph$	>10	2.277 ± 0.100
60	$NH(CH_2)_2OPh$	>10	>10
61	$NH(CH_2)_3CO_2H$	5.22 ± 0.38	0.568 ± 0.085
62	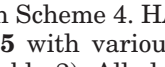	>10	0.610 ± 0.060

[a] Assay details were described in Experimental Section.

Results and Discussion

Lead Optimization. With 3-chloroanilino-pyrazine-pyridine-biheteroaryl **7**[25] as the VEGFR-2 lead molecule in hand (IC_{50} = 0.084 μM, Table 1), we first examined the binding affinities of other substituents at the upper-right position. While a smaller 3-fluoroanilino-pyrazine **11** (IC_{50} = 0.168 μM) reduced the binding affinity about 2-fold, the sterically bulkier 3-methoxyanilino-pyrazine **15** (IC_{50} = 0.74 μM) decreased the binding affinity almost 10-fold. Replacing the 3-chloroaniline of **7** with 2-chloroaniline reduced the potency about 12-fold (**19**, IC_{50} = 1.01 μM). In a parallel study, we found out that replacing the hydroxyl group in the lower side chain of **7** with a 4-pyridine ring gave compound **20** with comparable potency (IC_{50} = 0.076 μM). We thus synthesized two other analogues in compound **20** series in

Scheme 3[a]

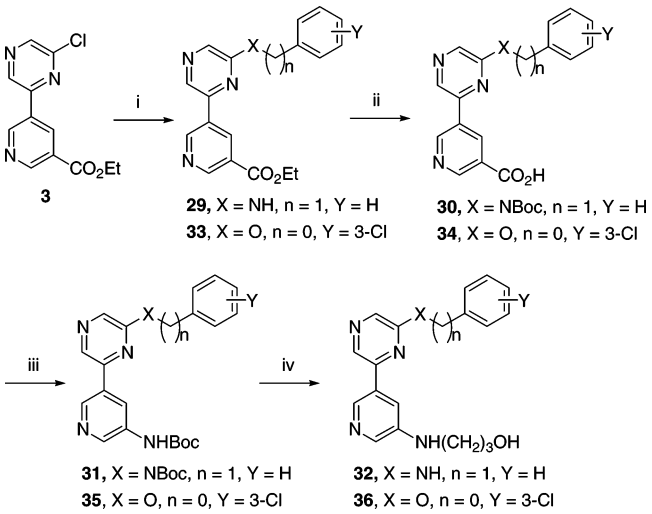

[a] (i) Benzylamine (or 3-chlorophenol), $Pd_2(dba)_3$, DPPF, Cs_2CO_3, 110 °C; (ii) (a) Boc_2O, DMAP, (b) NaOH, 0−20 °C (or NaOH, 0−20 °C); (iii) DPPA, Et_3N, *t*-BuOH, 65−100 °C; (iv) (a) $Br(CH_2)_3OTBS$, Cs_2CO_3, 70 °C, (b) TFA.

Scheme 4[a]

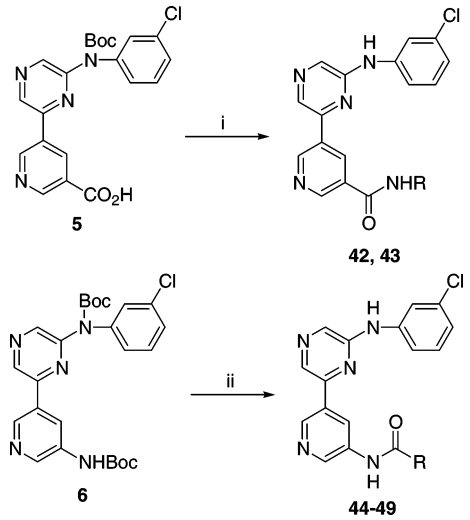

[a] (i) (a) $NH_2(CH_2)_nR$, DIPA, HATU, 20 °C, (b) TFA; (ii) (a) 60% NaH, R^1COCl, 20 °C, (b) TFA.

comparison to compound **7** series. Replacing the 3-chloroaniline of **20** with 4-chloroaniline reduced the potency about 13-fold (**24**, IC_{50} = 1.0 μM). On the other hand, replacement of the 3-chloroaniline of **20** with 3,4-dichloroaniline only decreased the potency about 2-fold (**28**, IC_{50} = 0.189 μM). These examples suggested that 3-chloro-substitution seems to be highly favorable to the binding affinity. In addition, replacement of the 3-chloroaniline of **7** with a benzylamine group also resulted in 13-fold lower potency (**32**, IC_{50} = 1.05 μM). Converting the 3-chloroaniline of **7** to a 3-chlorophenol moiety totally abolished the potency (**36**, IC_{50} >10 μM). These two examples further demonstrated the important contributions of 3-chloroaniline in the upper-right position to the inhibitory potency at VEGFR-2. Meanwhile, all of these compounds showed poor inhibition at CDK1 (IC_{50} >10 μM).

We next turned our attentions to the binding affinities of substituents at the lower-right position. Removal of the hydroxypropyl side chain of **7** gave **37** with 14-fold

Scheme 5[a]

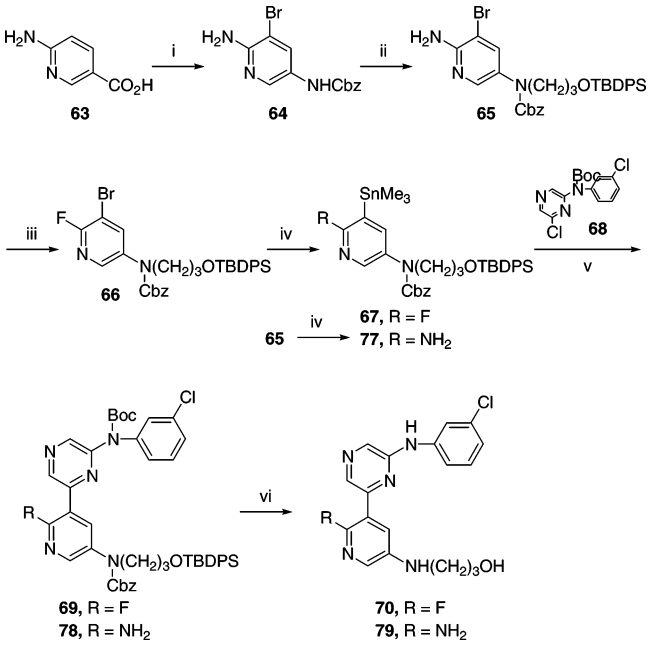

[a] (i) (a) Br_2, H_2O, (b) DPPA, Et_3N, $PhCH_2OH$; (ii) $Br(CH_2)_3OTBDPS$, Cs_2CO_3; (iii) $NOBF_4$; (iv) $Pd(PPh_3)_4$, Me_6Sn_2, LiCl, BHT; (v) **68**, $Pd(PPh_3)_2Cl_2$, LiCl; (vi) (a) H_2, 10%Pd/C, (b) TFA, CH_3SO_3H.

Scheme 6[a]

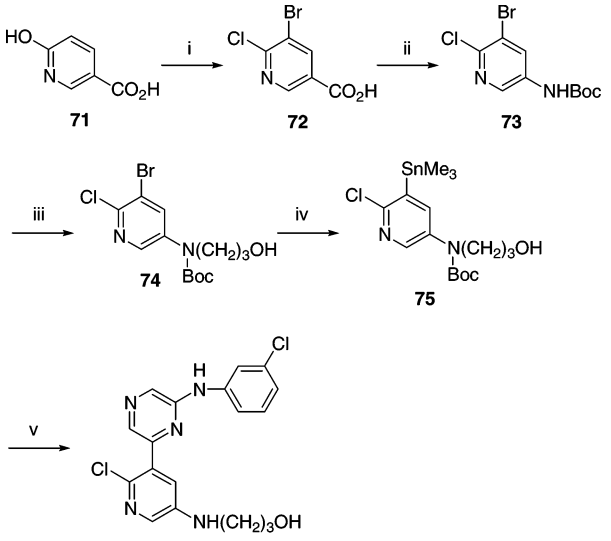

[a] (i) (a) Br_2, H_2O, (b) $POCl_3$, quinoline; (ii) DPPA, Et_3N, *t*-BuOH; (iii) $Br(CH_2)_3OH$, Cs_2CO_3; (iv) $Pd(PPh_3)_4$, Me_6Sn_2, LiCl, BHT; (v) **68**, $Pd(PPh_3)_2Cl_2$, LiCl.

reduced potency (**37**, IC_{50} = 1.16 μM, Table 2). Shortening the three-carbon side chain of **7** to a two-carbon side chain gave a 3-fold less potent compound (**38**, IC_{50} = 0.275 μM). Extending the three-carbon side chain to a four-carbon-chain provided a slightly more potent analogue (**39**, IC_{50} = 0.063 μM). Replacing the hydroxyl group of **7** with a dimethylamino group generated **40** with moderately lower potency (**40**, IC_{50} = 0.135 μM). Interestingly, shortening the three-carbon side chain of dimethylamino compound **40** to a two-carbon-chain analogue regained some of the potency (**41**, IC_{50} = 0.105 μM).

With no dramatic improvement in potency observed in amino side chain series (**38**−**41**), we decided to

explore the potency of the amide side chain series. Insertion of a carbonyl group between the biheteroaryl and the amino side chain of **41** or **7** gave the corresponding amide **42** ($IC_{50} = 4.3\ \mu M$) or amide **43** ($IC_{50} = 2.38\ \mu M$). The 41- and 28-fold decreased potencies of amide **42** (versus amine **41**) and amide **43** (versus amine **7**) might suggest the importance of a direct attachment of a NH moiety of the side chain to the biheteroaryl to the binding affinity.

Upon the basis of these observations, we felt the reversed-amide side chain series, with direct attachment of the NH moiety to the biheteroaryl, might be still worthy of investigation. We thus replaced one of the methylene units of **38** with a carbonyl group to generate reversed-amide **44**. Indeed, no dramatic loss of potency of **44** ($IC_{50} = 0.346\ \mu M$) was observed when compared to the amine **38** ($IC_{50} = 0.275\ \mu M$). Increasing the length of the side chain of **44** by adding one methylene unit to the hydroxyl end gave compound **45** ($IC_{50} = 0.303\ \mu M$) with slightly better potency. Further increasing the chain length of **45** by adding another methylene unit to the center of the side chain gave compound **46** ($IC_{50} = 0.593\ \mu M$) with 2-fold lower potency. We next examined the impact of an additional aromatic ring on the binding affinity. Replacement of the methoxy group of **45** with the benzyloxy group totally abolished the potency (**47**, $IC_{50} > 10\ \mu M$). Shortening the chain length by removing one methylene or two methylene units did not restore any potency (**48** and **49**, $IC_{50} > 10\ \mu M$). It seems that the installation of a phenyl group was detrimental to the binding affinity.

Since lower potencies were observed in both the amide and the reversed-amide series, we decided to revisit the amine side chain series. Incorporation of piperazine, morpholine, piperidine, and tetrahydropyran heterocycles to the side chain provided compounds **50**−**54** with IC_{50}'s ranging from 0.123 to 0.399 μM. On the other hand, we were pleased to find out that the incorporation of pyridine, pyrazole, and triazole heteroaryls to the side chain led to compounds **20** and **56**−**58** with good potency (**20**, $IC_{50} = 0.076\ \mu M$; **56**, $IC_{50} = 0.076\ \mu M$; **57**, $IC_{50} = 0.094\ \mu M$; **58**, $IC_{50} = 0.067\ \mu M$), although the four-carbon-chain analogue (**55**, $IC_{50} = 0.266\ \mu M$) was less favorable than the three-carbon-chain analogue (**20**, $IC_{50} = 0.076\ \mu M$). These results were particularly surprising considering the detrimental effect of phenyl incorporation in reversed-amide series, as shown in **47**−**49** ($IC_{50} > 10\ \mu M$). To confirm that the poor potencies of **47**−**49** were due to the phenyl group but not to the reversed-amide moiety, we synthesized compounds **59** and **60**. Indeed, the poor potency of **59** ($IC_{50} = 2.277\ \mu M$) and **60** ($IC_{50} > 10\ \mu M$) in the amine series further demonstrated that the phenyl ring, but not the heteroaryl ring, was unfavorable to the inhibition at VEGFR-2. Replacement of the hydroxyl group of **7** with carboxyl or carboxyamide gave **61** ($IC_{50} = 0.568\ \mu M$) or **62** ($IC_{50} = 0.61\ \mu M$) with 7-fold lower potency. All of the compounds prepared in Table 2 exhibit poor potency against CDK1.

Up to this point, our studies suggested that the NH unit of the lower side chain is critical to the binding affinity and might, potentially, serve as a hydrogen-bond donor site. Therefore, we attempted to adjust the hydrogen-bond donor capability of the NH moiety and thus the binding affinity of the molecule by increasing or decreasing the electron density in the pyridine ring. However, installation of an electron-withdrawing fluorine atom in the pyridine ring at the para position relative to the amino side chain gave compound **70** with 3-fold lower potency ($IC_{50} = 0.251\ \mu M$, Table 3) than compound **7** ($IC_{50} = 0.084\ \mu M$). Incorporation of an electron-donating amino group even further reduced the inhibitory potency to micromolar range (**79**, $IC_{50} = 1.36\ \mu M$). Replacement of the fluorine atom with an "electron neutral" but sterically bulkier chlorine atom totally abolished the potency (**76**, $IC_{50} > 10\ \mu M$). It appears that the hydrogen atom may still be the most favorable atom at this position.

Table 3. Binding Affinities at CDK1 and VEGFR-2[a]

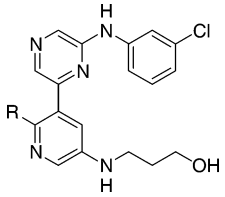

compd	R	$IC_{50} \pm$ SEM (μM) CDK1	$IC_{50} \pm$ SEM (μM) VEGFR-2
70	F	>10	0.251 ± 0.110
76	Cl	>10	>10
79	NH_2	>10	1.36 ± 0.65

Table 4. IC_{50} (μM) at Selected Kinase Assays[a]

kinase assay	**7**	**39**	**41**	**56**	**57**	**58**
VEGFR-2	0.084	0.063	0.105	0.076	0.094	0.067
calmodulin kinase-2	>10	>10	>10	>10	>10	>10
casein kinase-1	>10	>10	>10	>10	5.6	6.5
casein kinase-2	>10	>10	>10	>10	8.1	7.2
CDK1	>10	>10	>10	>10	>10	>10
CDK4	>10	>10	>10	ND[b]	ND	ND
EGFR	1.36	7.4	>10	>10	ND	ND
FGFR-2	0.21	2.36	1.40	0.293	0.326	0.153
GSK-3	0.478	4.02	>10	0.318	0.606	0.196
insulin R kinase	1.69	>10	>10	>10	>10	>10
MAPK	>10	>10	>10	>10	>10	>10
PDGF-R	0.36	2.8	>10	0.876	1.7	0.725
PKA	>10	>10	>10	>10	>10	>10
PKCβ2	>10	>10	>10	ND	ND	ND
PKCγ	>10	>10	3.96	ND	ND	ND

[a] Assay details were described in Experimental Section. IC_{50} values were reported as the average of at least two separate determinations. [b] ND: IC_{50} not determined because less than 50% inhibition was observed at 10 μM concentration of the compounds tested.

Kinase Selectivity

We next examined the selectivity of the most potent compounds in each subseries against a representative panel of kinases (Table 4). First, in the hydroxyalkylamino series, while the three-carbon-chain biheteroaryl **7** (VEGFR-2, $IC_{50} = 0.084\ \mu M$) showed very modest selectivity (2−6-fold) against fibroblast growth factor receptor kinase (FGFR-2, $IC_{50} = 0.21\ \mu M$), platelet-derived growth factor receptor kinase (PDGF-R, $IC_{50} = 0.36\ \mu M$), and glycogen synthase kinase-3 (GSK-3, $IC_{50} = 0.478\ \mu M$), it exhibited more than 1 order of magnitude of selectivity against epidermal growth factor receptor (EGFR, $IC_{50} = 1.36\ \mu M$) and insulin-R kinase ($IC_{50} = 1.69\ \mu M$). On the other hand, the four-carbon-chain analogue **39** (VEGFR-2, $IC_{50} = 0.063\ \mu M$) exhibited more than 1 order of magnitude of selectivity

Table 5. IC_{50} for Inhibition of Cell Proliferation[a]

cell line	IC_{50} (μM)					
	7	**39**	**41**	**56**	**57**	**58**
VEGF-stimulated HUVEC	0.164 ± 0.033	0.063 ± 0.033	0.059 ± 0.005	0.086 ± 0.008	0.120 ± 0.027	0.057 ± 0.014
HUVEC	1.68 ± 0.15	1.17 ± 0.37	0.877 ± 0.056	1.67 ± 0.16	1.39 ± 0.33	1.07 ± 0.05
HASMC	3.87 ± 0.17	3.23 ± 0.16	2.77 ± 0.06	6.15 ± 0.31	3.00 ± 0.08	2.98 ± 0.12
MRC5	6.60 ± 0.11	3.61 ± 0.15	2.91 ± 0.10	3.38 ± 0.09	3.61 ± 0.35	6.72 ± 0.09
HeLa	>10	5.56 ± 0.62	>10	3.06 ± 0.44	3.50 ± 0.16	6.06 ± 0.13
HCT-116	>10	>10	8.58 ± 0.67	5.05 ± 0.06	5.24 ± 0.19	>10
A375	>10	6.08 ± 0.48	3.72 ± 0.87	2.96 ± 0.05	2.84 ± 0.01	5.16 ± 0.03

[a] Assay details were described in Experimental Section.

against FGFR-2 (IC_{50} = 2.36 μM), PDGF-R (IC_{50} = 2.8 μM), and GSK-3 (IC_{50} = 4.02 μM), while it displayed more than 2 orders of magnitude of selectivity against EGFR (IC_{50} = 7.4 μM) and insulin-R kinase (IC_{50} >10 μM). Meanwhile, both compound **7** and compound **39** exhibited at least 2 orders of magnitude of selectivity against calmodulin kinase 2, casein kinase-1 or -2, CDK1, CDK4, mitogen-activated protein kinase (MAPK), protein kinase A (PKA), PKCβ2, and PKCγ (IC_{50} >10 μM).

Second, in the dimethylaminoalkyl-amino series, the two-carbon-chain biheteroaryl **41** (VEGFR-2, IC_{50} = 0.105 μM) showed more than 1 order of magnitude of selectivity against FGFR-2 (IC_{50} = 1.4 μM) and PKCγ (IC_{50} = 3.96 μM), meanwhile, it displayed at least 2 orders of magnitude of selectivity against the remaining 12 kinases (IC_{50} >10 μM). Third, in the six-membered heteroarylalkyl-amino series, the three-carbon-chain biheteroaryl **56** (VEGFR-2, IC_{50} = 0.076 μM) exhibited very modest selectivity (4−12-fold) against FGFR-2 (IC_{50} = 0.293 μM), GSK-3 (IC_{50} = 0.318 μM), and PDGF-R (IC_{50} = 0.876 μM), while it displayed at least 2 orders of magnitude of selectivity against the remaining 11 kinases (IC_{50} > 10 μM). Fourth, in the five-membered heteroarylalkyl-amino series, both of the three-carbon-chain biheteroaryls **57** and **58** exhibited very modest selectivity (2−18-fold) against FGFR-2, GSK-3, and PDGF-R, while both compounds displayed a more than 60-fold selectivity against casein kinase-1 and -2. Meanwhile, both compounds exhibited at least 2 orders of magnitude of selectivity against the remaining nine kinases (Table 4).

FGFR-2 and PDGF-R have been implicated indirectly in inducing VEGF secretion and hence angiogenesis.[32] ST1-571 (Gleevec) is a potent PDGF-R inhibitor and a v-Abl inhibitor. It has been approved recently for the treatment of chronic myeloid leukemia and KIT-positive metastatic malignant gastrointestinal stromal tumors and is under investigation in the treatment of glioblastomas, which exploits its PDGFR inhibitory activity.[33] Therefore, although we were targeting the VEGFR inhibition, the very modest selectivity of several of these compounds against FGFR-2 and PDGF-R may not be undesirable.

Cellular Selectivity

The cellular activity of the compound was tested for its ability to inhibit VEGF-stimulated proliferation of human umbilical vein endothelial cells (HUVEC). In hydroxyalkyl-amino series, while the three-carbon-chain biheteroaryl **7** exhibited submicromolar cellular potency (IC_{50} = 0.164 μM, Table 5) for inhibiting VEGF-stimulated proliferation, it only displayed a modest effect on the unstimulated growth of HUVEC (IC_{50} = 1.68 μM). The 10-fold difference in potency of compound **7** for inhibition of VEGF-stimulated versus unstimulated growth of HUVEC may suggest its specificity of action through inhibition of VEGFR signal transduction. Meanwhile, the four-carbon-chain analogue **39** also exhibited high cellular potency (IC_{50} = 0.063 μM) for inhibiting VEGF-stimulated proliferation, and therefore it displayed around 20-fold of selectivity against unstimulated growth of HUVEC (IC_{50} = 1.17 μM). Interestingly, compound **39** demonstrated consistently higher cellular selectivity and higher kinase selectivity than compound **7**. In addition, both compound **7** and compound **39** displayed very minimal inhibition of proliferation in two normal human cell types, human aortic smooth muscle cells (HASMC, IC_{50} = 3.87 μM for **7** and IC_{50} = 3.23 μM for **39**), and MRC5 lung fibroblasts (IC_{50} = 6.6 μM for **7** and IC_{50} = 3.61 μM for **39**). These data further indicate the high cellular selectivity of both compound **7** and compound **39** in VEGF-mediated processes.

Consistently, dimethylamino-biheteroaryl **41** and pyridine-biheteroaryl **56** displayed good cellular potency for inhibiting VEGF-stimulated HUVEC proliferation (IC_{50} = 0.059 μM for **41** and IC_{50} = 0.086 μM for **56**), while they maintained the lower potencies for inhibiting unstimulated growth of cell lines (IC_{50} ranging from 0.877 to 6.15 μM). Therefore, both compound **41** and **56** displayed more than 15-fold of cellular selectivity in general. Similarly, the pyrazole-biheteroaryl **57** and triazole-biheteroaryl **58** also exhibited higher cellular potencies for inhibiting VEGF-stimulated HUVEC proliferation (IC_{50} = 0.120 μM for **57** and IC_{50} = 0.057 μM for **58**) versus unstimulated growth of cell lines (IC_{50} ranging from 1.07 μM to >10 μM, Table 5).

The ability of all of these compounds to inhibit the proliferation of cells derived from carcinomas originating from various tissues such as HeLa (cervical adenocarcinoma), HCT-116 (colon carcinoma) and A375 (malignant melanoma) was also examined. The low inhibition of the growth of these tumor cell lines (IC_{50} ranging from 2.84 μM to >10 μM, Table 5) further confirms that these VEGFR inhibitors do not exhibit general cytotoxic antiproliferative activity as would occur through inhibition of growth regulatory kinases such as CDK1 inhibitors.

In Vivo Antitumor Activity

The antitumor activity of representative compounds[34a] **39** and **41** were evaluated against A375 human melanoma xenografts growing in nude mice,[34b] and the result is shown in Table 6, while the percent remaining survival plot is shown in Figure 2. Control groups

Table 6. In Vivo A375 Treatment Response Summary[a]

group	*n*	agent	mg/kg	MDS ± SEM (*n*) when reach 2.0 g	no death
1	10	growth control		20.6 ± 1.4 (10)	0
2	6	1.5% Pluronic F108		20.6 ± 2.1 (6)	0
3	6	1.5% Pluronic F108 and DTIC	90	24.5 ± 1.6 (6)	0
4	6	**39**	10	24.0 ± 1.2 (6)	0
5	6	**39**	75	29.2 ± 2.9 (6)	0
6	6	**41**	10	22.4 ± 1.2 (6)	0
7	6	**41**	75	28.9 ± 2.3 (6)	0

[a] Assay details were described in the Experimental Section.

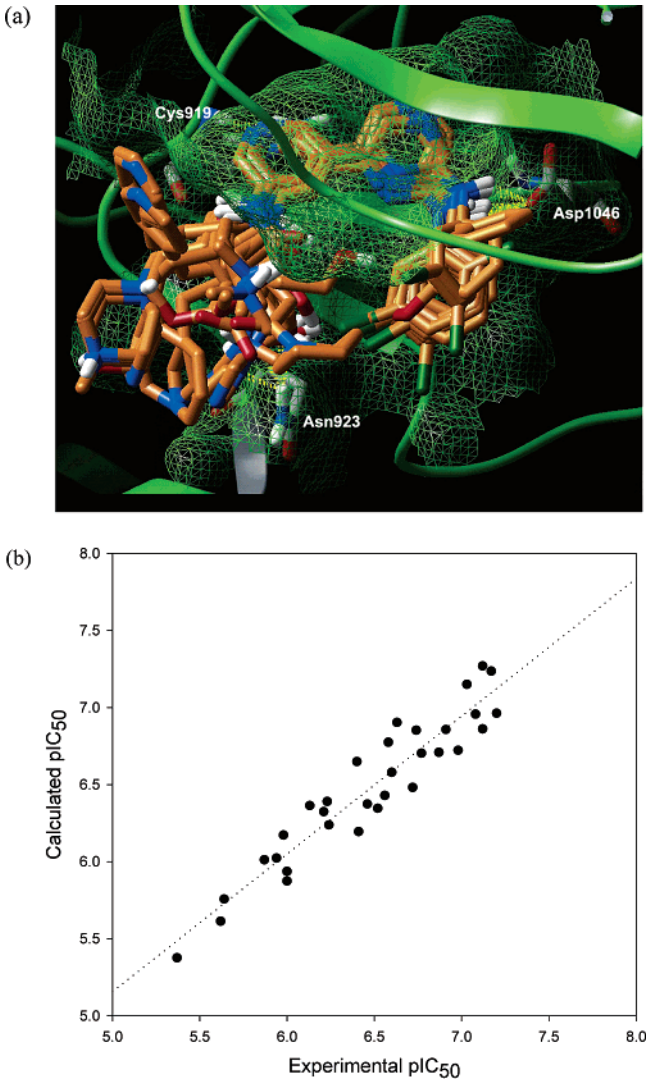

Figure 1. (a) Illustration of the alignment of 32 compounds in the ATP-binding site of VEGFR-2. The ligands and the key residues that act as their hydorgen-bond partners are represented in the tube model, while the protein is represented in the carton model. The hydrogen bonds are indicated by the yellow dotted lines. The connolly water-accessible surface of binding site is represented as meshes. (Atom color scheme: hydrogen in white; oxygen in red; nitrogen in blue; chlorine in dark green; carbon on ligands in orange; and carbon on proteins in gray.) (b) Correlation plot of the calculated pIC_{50} values from eq 1 versus the experimental pIC_{50} values. The dotted line represents the best fitting line between them.

included a no treatment tumor growth control group (10 mice, group 1), and a vehicle control group (6 mice, group 2). In addition, dacarbazine (DTIC), a cancer chemotherapy drug used in the treatment of melanoma

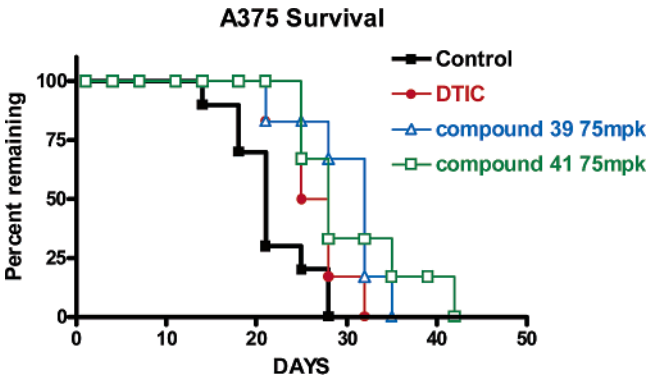

Figure 2. Compounds **39** and **41** delay tumor growth and increase survival in an A375 melanoma tumor xenograft model. Compounds were administered to nude mice IP at 75 mg/kg, and tumor growth was measured. Percent remaining refers to the number of animals remaining in the study with a tumor size under 2 g. Animals with a tumor size over 2 g were removed from the study but do not represent treatment-related deaths. Control animals were treated with vehicle alone (■). Dacarbazine (DTIC) was administered at 90 mg/kg on a qd × 5 schedule (red solid circles). Compound **39** (blue open triangles) and compound **41** (green open squares) were administered on a QD x 30 schedule, and the experiment was ended on day 60.

patients, was given i.p. at 90 mg/kg on a qd × 5 schedule to another group of mice as a positive-control group (group 3).[34c] Compound **39** or **41** was administered i.p. at either 10 mg/kg (group 4 or group 6) or 75 mg/kg (group 5 or group 7) on a qd × 30 schedule to two groups of mice. The tumor growth delay method was used in this study. Each animal was euthanized when its A375 neoplasm reached a size of 2.0 g. Mean day of survival (MDS) values were calculated for all groups. The MDS value of 29.2 days calculated from the compound **39**-treated animal group (75 mg/kg, group 5) is significant differently from the vehicle-control group (MDS = 20.6 days, $p = 0.05$) and represents a 41.7% ($p = 0.05$) survival increase. Similarly, the MDS value of 28.9 days calculated from the compound **41**-treated animal group (75 mg/kg, group 7) represents a 40.3% survival increase. In comparison, the MDS value of 24.5 days was obtained from the DTIC-treated animal group (group 3). All of these treatments with compound **39** or **41** were well tolerated; no animal deaths or weight losses were recorded. Therefore, it may be possible to administer higher dose of **39** or **41** to increase its moderate efficacy if desired.

Molecular Modeling Studies

A QSAR analysis was conducted in an attempt to rationalize the observed structure−activity data. On the basis of the previously developed model of VEGFR-2 in complex with **7**,[25] all the 32 compounds with IC_{50} values less than 10 μM in Tables 1−3 were docked into the ATP-binding site of VEGFR-2, using the docking program Glide.[39] The favorable docking poses were then used to develop QSAR models. The binding poses were finally predicted as those leading to the best QSAR model (see Experimental Section. Computational Details). Their alignment in the binding pocket is illustrated in Figure 1a. Generally, they all adopt a unique hydrogen-bond pattern to interact with VEGFR-2: one hydrogen bond between the pyridine nitrogen

and the backbone amide nitrogen of Cys919 at the so-called hinge region and the other between the anilino nitrogen and the side chain carboxylate group of Asp1046. In addition, some compounds with a polar group on their aliphatic side chains may pick up some hydrogen-bond interactions with Asn923.

The QSAR analysis was carried out with the GlideScore[40] components. GlideScore is a popular empirical scoring function that estimates binding affinity as the sum of multiple empirical terms. The relative contribution of each term can be determined by fitting to the known experimental data of binding affinity. By retraining them in our data set of 32 compounds, the following regression model was obtained as optimal using five GlideScore components.

$$\mathrm{pIC_{50}} = 3.366 \times \mathrm{Lipo} - 4.805 \times \mathrm{BuryP} - 0.244 \times \mathrm{vdW} - 0.109 \times \mathrm{Coul} + 1.889 \times \mathrm{Site} + 5.081 \quad (1)$$

in which $n = 32$, rmsd = 0.160, $r^2 = 0.894$, $q^2 = 0.851$.

Here, Lipo represents the lipophilic contact term that counts the favorable hydrophobic−hydrophobic matches between the ligand and the receptor. BuryP is the penalty term that counts the unfavorable mismatches of polar or charged groups in a hydrophobic binding pocket. It actually provides a way to take into account the solvation effect in binding. vdW and Coul represent the contributions from the van der Waals and Coulomb interaction energies between the ligand and the receptor, respectively. Site is the reward term that considers polar but non-hydrogen-bonding atoms found in a hydrophobic pocket. The other GlideScore components were discarded because their inclusion actually made the model worse.

For 32 compounds, eq 1 produces a conventional correlation coefficient r^2 of 0.894 and a leave-one-out cross-validated correlation coefficient q^2 of 0.851. The root-mean-square deviation (rmsd) is 0.160. These values clearly indicate this model as a statistically significant and stable model. The r^2 value of 0.894 also indicates that this model can explain approximately 89.4% of the internal variance observed in the experimental pIC50 data. The calculated and the experimental $\mathrm{pIC_{50}}$ values are listed in Table 7 and plotted in Figure 1b.

The two major contributions are from the Lipo and vdW terms. They count 32.7 and 32.1% to the information content of this model, respectively. These numbers indicate that the complementary shape contacts between the ligand and the receptor, especially the hydrophobic−hydrophobic contacts, are the major differential force behind the VEGFR-2 binding of this series of compounds. Interestingly, the hydrogen-bond interaction term does not appear in the final model, although it obviously plays an important role in determining the binding poses of these compounds. This fact indicates that the optional hydrogen bonds with Asn923 are not directly involved in determining the variance of binding affinities within this series. Instead, they may contribute by influencing the binding poses of these compounds.

Table 7. Experimental and Calculated $\mathrm{pIC_{50}}$ Values, with the Values of the Five GlideScore Components Used in the Final QSAR Model

	GlideScore components					$\mathrm{pIC_{50}}$	
compound	Lipo	BuryP	vdW	Coul	Site	expt	calc
7	−2.48	0.00	−34.85	−15.73	0.00	7.08	6.96
11	−2.46	0.00	−33.87	−14.98	0.00	6.77	6.70
15	−2.47	0.00	−33.61	−12.75	0.00	6.13	6.36
19	−2.51	−0.90	−33.78	−11.24	−0.09	6.00	5.94
20	−2.75	0.00	−40.04	−11.54	0.00	7.12	6.86
24	−2.90	0.00	−39.92	−7.38	0.00	6.00	5.87
28	−3.24	0.00	−45.42	−11.13	0.00	6.72	6.48
32	−2.61	0.00	−33.86	−14.76	0.00	5.98	6.17
37	−2.25	0.00	−31.67	−7.16	0.00	5.94	6.02
38	−2.48	0.00	−35.41	−9.62	0.00	6.56	6.43
39	−2.57	0.00	−36.34	−15.22	0.00	7.20	6.96
40	−2.62	0.00	−36.64	−13.76	0.00	6.87	6.71
41	−2.59	0.00	−36.78	−12.64	0.00	6.98	6.72
42	−2.48	0.20	−37.73	−10.51	−0.40	5.37	5.38
43	−2.53	0.20	−40.08	−10.00	−0.46	5.62	5.61
44	−2.45	0.00	−37.03	−12.36	−0.45	6.46	6.37
45	−2.46	0.00	−37.71	−10.71	−0.44	6.52	6.35
46	−2.51	0.00	−38.69	−10.81	−0.46	6.23	6.39
50	−2.74	0.00	−39.84	−12.07	0.00	6.63	6.90
51	−2.75	0.00	−39.84	−11.96	0.00	6.91	6.86
52	−2.73	0.00	−40.07	−10.78	0.00	6.74	6.85
53	−2.79	0.00	−39.37	−12.34	0.00	6.40	6.65
54	−2.83	0.00	−38.80	−10.68	0.00	6.41	6.20
55	−2.92	0.00	−40.89	−14.10	0.00	6.58	6.77
56	−2.67	0.00	−39.89	−13.16	0.00	7.12	7.27
57	−2.66	0.00	−39.80	−11.96	0.00	7.03	7.15
58	−2.57	0.00	−38.90	−11.98	0.00	7.17	7.24
59	−3.30	0.00	−43.64	−10.33	0.00	5.64	5.76
61	−2.58	0.00	−35.96	−9.72	0.00	6.24	6.24
62	−2.73	0.00	−39.73	−6.69	0.00	6.21	6.32
70	−2.38	0.00	−35.60	−13.21	−0.33	6.60	6.58
79	−2.53	0.00	−35.37	−14.02	−0.38	5.87	6.01

Conclusion

Using palladium-catalyzed C−C bond, C−N bond formation reactions as the key methods, SAR studies of the pyrazine-pyridine lead were conducted. These efforts resulted in the identification of several potent VEGFR-2 inhibitors with various degrees of kinase selectivity. Among them, compound **39** and compound **41** exhibited the highest kinase selectivity, while compound **7** and compounds **56**−**58** displayed modest selectivity against FGFR-2, PDGF-R, and GSK-3. All of these compounds showed high cellular potency to inhibit VEGF-stimulated proliferation of HUVEC. Meanwhile, they all displayed modest effect on the unstimulated growth of HUVEC and very minimal inhibition of proliferation of two normal human cell types, HASMC and MRC5. The low inhibition of these compounds to the growth of tumor cell lines, such as HeLa, HCT-116, and A375 further confirms that these VEGFR-2 inhibitors are not cytotoxic agents. The in vivo antitumor activity of compounds **39** and **41** was demonstrated in the A375 human melanoma xenograft nude mice model. Molecular modeling (QSAR analysis) was conducted in an attempt to rationalize the observed SAR. The high VEGFR-2 inhibitory potency, good kinase selectivity profile, and good cellular potency and selectivity demonstrated in vivo antitumor activity may potentially render these compounds as valuable pharmacological tools in elucidating the complex roles of VEGF signaling pathways and the potential utility for anti-angiogenesis therapy.

Experimental Section

Chemistry. ^{1}H NMR spectra were measured on a Bruker AC-300 (300 MHz) spectrometer using tetramethylsilane as an internal standard. Elemental analyses were obtained by

Quantitative Technologies Inc. (Whitehouse, New Jersey), and the results were within 0.4% of the calculated values unless otherwise mentioned. Melting points were determined in open capillary tubes with a Thomas-Hoover apparatus and were uncorrected. The optical rotation was measured at 25 °C with an Autopol III polarimeter. Electrospray mass spectra (MS-ES) were recorded on a Hewlett-Packard 59987A spectrometer. High-resolution mass spectra (HRMS) were obtained on a Micromass Autospec. E. spectrometer. The term DMAP refers to (dimethylamino)pyridine, TFA refers to trifluoroacetic acid, NMP refers to 1-methyl-2-pyrrolidinone, DPPF refers to 1,1′-bis(diphenylphosphino)ferrocene, $Pd_2(dba)_3$ refers to tris(dibenzylideneacetone)dipalladium(0)-chloroform adduct, and DPPA refers to diphenylphosphoryl azide.

5-Tributylstannanyl-nicotinic Acid Ethyl Ester 2. A mixture of 5-bromonicotinate **1** (25 g, 108.7 mmol), bis(tributyltin) (63.05 g, 108.7 mmol), palladium acetate (1.1 g, 4.89 mmol), tri-*o*-tolylphosphine (8.6 g, 28.26 mmol), and triethylamine (21.96 g, 217.4 mmol) in acetonitrile (350 mL) was stirred at 95−100 °C for 22 h under nitrogen. The cooled reaction mixture was filtered through Celite. Then the Celite was washed with more acetonitrile, and the combined acetonitrile was concentrated under a vacuum. The residue was diluted with a suitable solvent, such as dichloromethane, washed with aqueous sodium carbonate and concentrated. The residue was further diluted with hexane. The solid was filtered off, and the filtrate was concentrated. The product was purified by column chromatography (twice, SiO_2, dichloromethane/hexane as solvent) to give 19.09 g (40%) of **2** as a light orange oil: ^{1}H NMR (300 MHz, $CDCl_3$) δ 9.11 (brs, 1 H), 8.74 (brs, 1 H), 8.35 (brs, 1 H), 4.41 (q, J = 6.9 Hz, 2 H), 1.72−1.05 (m, 21 H), 0.89 (t, J = 7.2 Hz, 9 H); MS (ES) *m/z*: 442 (M + H$^+$).

5-(6-Chloro-pyrazine-2-yl)-nicotinic Acid Ethyl Ester 3. A mixture of **2** (10 g, 22.7 mmol), 2,6-dichloropyrazine (6.76 g, 45.4 mmol), dichloro-bis(triphenylphosphine)palladium (797 mg, 1.14 mmol), and LiCl (4.77 g, 113.5 mmol) in anhydrous toluene (85 mL) was stirred at 100 °C for 23 h under nitrogen. The cooled reaction mixture was concentrated under a vacuum. Aqueous sodium carbonate was added to the residue and stirred for 10 min and extracted with dichloromethane (3×). The combined dichloromethane solution was filtered through Celite, dried (Na_2SO_4), and concentrated. The product was purified by column chromatography (EtOAc/hexane as solvent) to give 3.56 g (60%) of **3** as an off-white solid: ^{1}H NMR (300 MHz, $CDCl_3$) δ 9.43 (brs, 1 H), 9.35 (brs, 1 H), 9.05 (s, 1 H), 8.91 (s, 1 H), 8.64 (s, 1 H), 4.48 (q, J = 7.3 Hz, 2 H), 1.47 (t, J = 7.2 Hz, 3 H); MS (ES) *m/z*: 264 (M+H$^+$). Anal. ($C_{12}H_{10}N_3O_2Cl$) C, H, N.

General Procedure for the Synthesis of 4, 8, 12, 16, 21, and 25. 5-[6-(3-Chloro-phenylamino)-pyrazin-2-yl]-nicotinic acid ethyl ester **4**. A mixture of **3** (24.3 g, 92.4 mmol), 3-chloroaniline (16.6 g, 129 mmol), $Pd_2(dba)_3$ (2.39 g, 2.31 mmol), DPPF (4.1 g, 7.4 mmol), and Cs_2CO_3 (60.2 g, 185 mmol) in anhydrous dioxane (230 mL) was stirred at 110 °C for 46 h under nitrogen. Dichloromethane (100 mL) was added to the cooled reaction mixture. The mixture was then filtered through Celite, the Celite cake was washed with more dichloromethane, and the combined filtrate was concentrated to give a yellow-brown solid. Small amounts of dichloromethane was added, the solid was collected through filtration, and the filtrate was concentrated. The solid collected was recrystallized from EtOAc/hexane to give 21.83 g (67%) of compound **4** as a yellow solid: ^{1}H NMR (300 MHz, $CDCl_3$) δ 9.44 (brs, 1 H), 9.31 (brs, 1 H), 8.90 (s, 1 H), 8.57 (s, 1 H), 8.26 (s, 1 H), 7.72 (s, 1 H), 7.44 (d, J = 8.1 Hz, 1 H), 7.31 (t, J = 8.0 Hz, 1 H), 7.08 (d, J = 8.0 Hz, 1 H), 7.04 (s, 1 H), 4.48 (q, J = 7.2 Hz, 2 H), 1.46 (t, J = 7.0 Hz, 3 H); MS (ES) *m/z*: 355 (M + H$^+$). Anal. ($C_{18}H_{15}N_4O_2Cl$) C, H, N.

General Procedure for the Synthesis of 5, 9, 13, 17, 22, and 26. 5-{6-[*tert*-Butoxycarbonyl-(3-chloro-phenyl)-amino]-pyrazin-2-yl}-nicotinic Acid 5. A mixture of **4** (21.83 g, 61.7 mmol), Boc_2O (26.9 g, 123 mmol), and DMAP (3 g, cat.) in dichloromethane (500 mL) was stirred at 20 °C for 4 h. The reaction mixture was concentrated, and the product was purified by column chromatography (EtOAc/hexane as solvent) to give 26.7 g (95%) of **Boc-4** as yellowish oil: ^{1}H NMR (300 MHz, $CDCl_3$) δ 9.22 (d, J = 2.0 Hz, 1 H), 9.15 (d, J = 2.2 Hz, 1 H), 9.10 (s, 1 H), 8.84 (s, 1 H), 8.64 (t, J = 2.1 Hz, 1 H), 7.35 (m, 3 H), 7.18 (brd, J = 7.3 Hz, 1 H), 4.44 (q, J = 7.1 Hz, 2 H), 1.50 (s, 9 H), 1.44 (t, J = 7.1 Hz, 3 H); MS (ES) *m/z*: 455 (M + H$^+$).

Compound **Boc-4** (32.2 g, 71 mmol) was dissolved in methanol (200 mL) and stirred for 10 min and then cooled to 0 °C. A $NaOH_{(aq)}$ (1 N, 118 mL) solution was added slowly, and the mixture was stirred at 0 °C for 20 min and then stirred at 20 °C for another 18 h. Glacial acetic acid (95 mL) was added to the reaction mixture at 0 °C slowly followed by the addition of water (350 mL). A yellow solid was formed. The yellow solid was collected through filtration, washed with water (5×), dried in a vacuum oven overnight to give 28.3 g (94%) of the carboxylic acid **5** as a yellow solid: ^{1}H NMR (300 MHz, DMSO-d_6) δ 9.27 (d, J = 1.9 Hz, 1 H), 9.22 (s, 1 H), 9.09 (d, J = 1.6 Hz, 1 H), 9.03 (s, 1 H), 8.65 (brs, 1 H), 7.52−7.31 (m, 4 H), 1.44 (s, 9 H); MS (ES) *m/z*: 425 (M−H$^+$). Anal. ($C_{21}H_{19}N_4O_4Cl$) C, H, N.

General Procedure for the Synthesis of 6, 10, 14, 18, 23, and 27. [6-(5-*tert*-Butoxycarbonylamino-pyridin-3-yl)-pyrazin-2-yl]-(3-chloro-phenyl)-carbamic Acid *tert*-Butyl Ester 6. A mixture of the carboxylic acid **5** (28.3 g, 66.5 mmol), DPPA (21.95 g, 80 mmol), triethylamine (13.43 g, 133 mmol), *t*-BuOH (280 mL) in toluene (200 mL) was stirred under nitrogen at 70 °C for 30 min and then stirred at 100 °C for 4 h. The reaction mixture was concentrated under a vacuum. The product was purified by column chromatography (EtOAc/hexane as solvent) to give 29.28 g (89%) of **6** as a yellowish foam: ^{1}H NMR (300 MHz, $CDCl_3$) δ 8.99 (s, 1 H), 8.80 (s, 1 H), 8.67 (d, J = 1.7 Hz, 1 H), 8.49 (d, J = 2.4 Hz, 1 H), 8.41 (brs, 1 H), 7.29 (m, 3 H), 7.17 (d, J = 7.5 Hz, 1 H), 7.08 (s, 1 H), 1.54 (s, 9 H), 1.49 (s, 9 H); MS (ES) *m/z*: 498 (M + H$^+$). Anal. ($C_{25}H_{28}N_5O_4Cl$) C, H, N.

General Procedure for the Synthesis of 7, 11, 15, and 19. 3-[[5-[6-[(3-chlorophenyl)amino]pyrazinyl]-3-pyridinyl]amino]-1-propanol 7. A mixture of **6** (3 g, 6 mmol), (3-bromopropoxy)-*tert*-butyl-dimethylsilane (2.28 g, 9 mmol) and Cs_2CO_3 (5.9 g, 18 mmol) in DMF (60 mL) was stirred at 70 °C under nitrogen for 36 h. The reaction mixture was diluted with water, extracted with ether (3×), dried (Na_2SO_4), and concentrated. The product was purified by column chromatography (EtOAc/hexane as solvent) to give 3.04 g of the silylated product as an orange oil. The silylated product was dissolved in TFA (30 mL) and stirred at 20 °C for 1 h before it was concentrated. An ammonium hydroxide solution was added to the residue until the pH was about 10−11, water was added, and a yellow solid was formed. The yellow solid was collected through filtration, washed with water, and dried under a vacuum. The yellow solid was recrystallized from CH_3OH/EtOAc to give 1.25 g (59%) of **7** as a light yellow solid: ^{1}H NMR (300 MHz, CD_3OD) δ 8.45 (s, 1 H), 8.41 (d, J = 1.6 Hz, 1 H), 8.12 (brs, 2 H), 8.00 (d, J = 2.7 Hz, 1 H), 7.66 (brs, 1 H), 7.55 (d, J = 8.3 Hz, 1 H), 7.30 (t, J = 8.1 Hz, 1 H), 6.99 (d, J = 7.9 Hz, 1 H), 3.72 (t, J = 6.3 Hz, 2 H), 3.33 (t, J = 6.8 Hz, 2 H), 1.91 (m, 2 H); MS (ES) *m/z*: 356 (M + H$^+$). Anal. ($C_{18}H_{18}N_5OCl\cdot0.5\ H_2O$) C, H, N.

5-[6-(3-Fluoro-phenylamino)-pyrazin-2-yl]-nicotinic Acid Ethyl Ester 8. Replacing 3-chloroaniline with 3-fluoroaniline and following the same procedure as in the preparation of **4** gave **8** as a yellow solid: 80% yield; ^{1}H NMR (300 MHz, $CDCl_3$) δ 9.42 (d, J = 2.2 Hz, 1 H), 9.30 (d, J = 2.0 Hz, 1 H), 8.91 (t, J = 2.1 Hz, 1 H), 8.58 (s, 1 H), 8.26 (s, 1 H), 7.54 (d, J = 10.9 Hz, 1 H), 7.38−7.24 (m, 1 H), 6.91 (s, 1 H), 6.83 (t, J = 8.1 Hz, 1 H), 4.48 (q, J = 7.1 Hz, 2 H), 1.46 (t, J = 7.1 Hz, 3 H); MS (ES) *m/z*: 339 (M + H$^+$).

5-{6-[*tert*-Butoxycarbonyl-(3-fluoro-phenyl)-amino]-pyrazin-2-yl}-nicotinic Acid 9. Replacing **4** with **8** and following the same procedure as in the preparation of **5** gave **9** as a yellow solid: 67% yield; ^{1}H NMR (300 MHz, $CDCl_3$) δ 9.29 (brs, 1 H), 9.20 (brs, 1 H), 9.13 (brs, 1 H), 8.86 (brs, 1 H),

8.73 (brs, 1 H), 7.44−7.27 (m, 1 H), 7.07−6.91 (m, 3 H), 1.50 (s, 9 H); MS (ES) *m/z*: 409 (M − H^+).

[6-(5-*tert*-Butoxycarbonylamino-pyridin-3-yl)-pyrazin-2-yl]-(3-fluoro-phenyl)-carbamic Acid *tert*-Butyl Ester 10. Replacing **5** with **9** and following the same procedure as in the preparation of **6** gave **10** as a yellowish gum: 31% yield; ^{1}H NMR (300 MHz, $CDCl_3$) δ 8.99 (s, 1 H), 8.80 (s, 1 H), 8.68 (d, J = 1.9 Hz, 1 H), 8.46 (d, J = 2.5 Hz, 1 H), 8.38 (brs, 1 H), 7.41−7.27 (m, 1 H), 7.06−7.01 (m, 3 H), 6.58 (brs, 1 H), 1.54 (s, 9 H), 1.49 (s, 9 H); FAB-HRMS (M + H^+) calcd. for $C_{25}H_{29}N_5O_4F$ 482.2204, found 482.2204.

3-[[5-[6-[(3-Fluorophenyl)amino]pyrazinyl]-3-pyridinyl]-amino]-1-propanol 11. Replacing **6** with **10** and following the same procedure as in the preparation of **7** gave **11** as a yellow solid: 27% yield; ^{1}H NMR (300 MHz, CD_3OD) δ 8.46 (s, 1 H), 8.43 (d, J = 1.8 Hz, 1 H), 8.13 (brs, 1 H), 8.01 (d, J = 2.7 Hz, 1 H), 7.90 (dt, J = 12.1, 2.1 Hz, 1 H), 7.68 (t, J = 2.1 Hz, 1 H), 7.42−7.28 (m, 2 H), 6.73 (t, J = 8.3 Hz, 1 H), 3.72 (t, J = 6.2 Hz, 2 H), 3.31 (m, 2 H), 1.91 (m, 2 H); FAB-HRMS (M + H^+) calcd. for $C_{18}H_{19}N_5OF$ 340.1574, found 340.1586.

5-[6-(3-Methoxy-phenylamino)-pyrazin-2-yl]-nicotinic Acid Ethyl Ester 12. Replacing 3-chloroaniline with 3-methoxyaniline and following the same procedure as in the preparation of **4** gave **12** as a yellow solid: 65% yield; ^{1}H NMR (300 MHz, $CDCl_3$) δ 9.42 (d, J = 2.1 Hz, 1 H), 9.28 (d, J = 2.0 Hz, 1 H), 8.89 (t, J = 2.1 Hz, 1 H), 8.53 (s, 1 H), 8.27 (s, 1 H), 7.3−7.27 (m, 2 H), 7.05 (dd, J = 7.9, 1.3 Hz, 1 H), 6.78 (brs, 1 H), 6.69 (brd, J = 7.6 Hz, 1 H), 4.48 (q, J = 7.1 Hz, 2 H), 3.85 (s, 3 H), 1.56 (t, J = 7.1 Hz, 3 H); Anal. ($C_{19}H_{18}N_4O_3 \cdot 0.5H_2O$) C, H, N.

5-{6-[*tert*-Butoxycarbonyl-(3-methoxy-phenyl)-amino]-pyrazin-2-yl}-nicotinic Acid 13. Replacing **4** with **12** and following the same procedure as in the preparation of **5** gave **13** as a yellow solid: 71% yield; ^{1}H NMR (300 MHz, CD_3OD) δ 9.16 (d, J = 2.2 Hz, 1 H), 9.11 (d, J = 1.9 Hz, 1 H), 9.04 (s, 1 H), 8.98 (s, 1 H), 8.82 (t, J = 2.1 Hz, 1 H), 7.35 (t, J = 8.0 Hz, 1 H), 6.96−6.85 (m, 3 H), 3.81 (s, 3 H), 1.48 (s, 9 H); MS (ES) *m/z*: 421 (M − H^+). Anal. ($C_{22}H_{22}N_4O_5 \cdot 0.3\ H_2O$) C, H, N.

[6-(5-*tert*-Butoxycarbonylamino-pyridin-3-yl)-pyrazin-2-yl]-(3-methoxy-phenyl)-carbamic Acid *tert*-Butyl Ester 14. Replacing **5** with **13** and following the same procedure as in the preparation of **6** gave **14** as a yellowish gum: 75% yield; ^{1}H NMR (300 MHz, $CDCl_3$) δ 8.91 (s, 1 H), 8.78 (s, 1 H), 8.71 (d, J = 1.9 Hz, 1 H), 8.49 (d, J = 2.5 Hz, 1 H), 8.38 (brs, 1 H), 7.31 (t, J = 8.2 Hz, 1 H), 6.87−6.82 (m, 3 H), 6.63 (brs, 1 H), 3.81 (s, 3 H), 1.54 (s, 9 H), 1.49 (s, 9 H); MS (ES) *m/z*: 494 (M + H^+).

3-[[5-[6-[(3-Methoxyphenyl)amino]pyrazinyl]-3-pyridinyl]amino]-1-propanol 15. Replacing **6** with **14** and following the same procedure as in the preparation of **7** gave **15** as a yellow solid: 10% yield; ^{1}H NMR (300 MHz, CD_3OD) δ 8.44 (d, J = 1.6 Hz, 1 H), 8.39 (s, 1 H), 8.10 (s, 1 H), 8.00 (d, J = 2.8 Hz, 1 H), 7.67 (brs, 1 H), 7.65 (brs, 1 H), 7.23−7.20 (m, 2 H), 6.62−6.58 (m, 1 H), 3.81 (s, 3 H), 3.72 (t, J = 6.2 Hz, 2 H) 3.31 (m, 2 H), 1.90 (m, 2 H); Anal. ($C_{19}H_{21}N_5O_2 \cdot 0.5\ H_2O$) C, H, N.

5-[6-(2-Chloro-phenylamino)-pyrazin-2-yl]-nicotinic Acid Ethyl Ester 16. Replacing 3-chloroaniline with 2-chloroaniline and following the same procedure as in the preparation of **4** gave **16** as a solid: 69% yield; ^{1}H NMR (300 MHz, $CDCl_3$) δ 9.44 (d, J = 3.0 Hz, 1 H), 9.30 (d, J = 3.0 Hz, 1 H), 8.89 (s, 1 H), 8.60 (s, 1 H), 8.37 (d, J = 9.0, 1 H), 8.29 (s, 1 H), 7.47 (d, J = 9.0, 1 H), 7.35 (dd, J = 9.0, 6.0 Hz, 1 H), 7.14 (brs, 1 H), 7.06 (dd, J = 9.0, 6.0 Hz, 1 H), 4.48 (q, J = 6.0 Hz, 2 H), 1.46 (t, J = 6.0 Hz, 3 H); MS (ES) *m/z*: 355 (M + H^+).

5-{6-[*tert*-Butoxycarbonyl-(2-chloro-phenyl)-amino]-pyrazin-2-yl}-nicotinic Acid 17. Replacing **4** with **16** and following the same procedure as in the preparation of **5** gave **17** as a solid: 64% yield as a mixture of two inseparable compounds (**17** and **des-Boc-17)** in 7:3 ratio; MS (ES) *m/z*: 427 (M + H^+).

[6-(5-*tert*-Butoxycarbonylamino-pyridin-3-yl)-pyrazin-2-yl]-(2-chloro-phenyl)-carbamic acid *tert*-butyl Ester 18. Replacing **5** with **17** and following the same procedure as in the preparation of **6** gave **18**: 50% yield; ^{1}H NMR (300 MHz, $CDCl_3$) δ 9.28 (s, 1 H), 8.74 (s, 1 H), 8.59 (d, J = 3 Hz, 1 H), 8.47 (d, J = 3.0 Hz, 1 H), 8.30 (brs, 1 H), 7.49 (dd, J = 9.0, 3.0 Hz, 1 H), 7.40−7.25 (m, 3 H), 6.98 (s, 1 H), 1.54 (s, 9 H), 1.47 (s, 9 H); MS (ES) *m/z*: 498 (M + H^+).

3-{5-[6-(2-Chloro-phenylamino)-pyrazin-2-yl]-pyridin-3-ylamino}-propan-1-ol 19. Replacing **6** with **18** and following the same procedure as in the preparation of **7** gave **19** as a solid: 61% yield; ^{1}H NMR (300 MHz, CD_3OD) δ 8.45 (s, 1 H), 8.36 (s, 1 H), 8.22 (s, 1 H), 8.17 (dd, J = 9.0, 3.0 Hz, 1 H), 7.97 (s, 1 H), 7.59 (s, 1 H), 7.47 (dd, J = 9.0, 3.0 Hz, 1 H), 7.34 (dd, J = 6.0, 6.0, 3.0 Hz, 1 H), 7.10 (ddd, J = 6.0, 6.0, 3.0 Hz, 1 H), 3.70 (t, J = 6.0 Hz, 2 H), 3.27 (t, J = 6.0 Hz, 2 H), 1.87 (t, J = 6.0 Hz, 2 H); MS (ES) *m/z*: 356 (M + H^+).

General Procedure for the Synthesis of 20, 24, and 28. (3-Chloro-phenyl)-{6-[5-(3-pyridin-4-yl-propylamino)-pyridin-3-yl]-pyrazin-2-yl}-amine 20. A mixture of **6** (0.1 g, 0.2 mmol), 4-(3-chloropropyl)pyridine[35] (0.047 g, 0.3 mmol), and Cs_2CO_3 (0.197 g, 0.6 mmol) in DMF (4 mL) was stirred at 70 °C under nitrogen for 20 h. The reaction mixture was diluted with water, extracted with ether (3×), dried (Na_2SO_4), and concentrated. The product was purified by column chromatography (EtOAc/MeOH as solvent) to give 0.074 g of product as an oil. The oil was dissolved in TFA (2.0 mL) and stirred at 20 °C for 2 h before concentrated. Ammonium hydroxide solution was added to the residue until the pH was about 10−11. The aqueous layer was extracted with CH_2Cl_2, dried (Na_2SO_4), and concentrated. Product was purified by column chromatography (CH_2Cl_2/MeOH as solvent) to give 0.045 g (91%) of **20** as a yellow solid: ^{1}H NMR (300 MHz, CD_3OD) δ 8.42 (m, 4 H), 8.12 (s, 2 H), 7.99 (s, 1 H), 7.65 (s, 1 H), 7.48 (m, 1 H), 7.34 (s, 2 H), 7.25 (t, J = 8.0 Hz, 1 H), 6.97 (d, J = 6.7 Hz, 1 H), 3.30 (m, 2 H), 2.83 (m, 2 H), 2.03 (m, 2 H); MS (ES) *m/z*: 417 (M + H^+); FAB-HRMS (M + H^+) calcd. for $C_{23}H_{22}ClN_6$ 417.1594, found 417.1605.

5-[6-(4-Chloro-phenylamino)-pyrazin-2-yl]-nicotinic Acid Ethyl Ester 21. Replacing 3-chloroaniline with 4-chloroaniline and following the same procedure as in the preparation of **4** gave **21** as a yellow solid: 56% yield; ^{1}H NMR (300 MHz, $CDCl_3$) δ 9.40 (d, J = 2.1 Hz, 1 H), 9.29 (d, J = 1.9 Hz, 1 H), 8.87 (t, J = 2.0 Hz, 1 H), 8.55 (s, 1 H), 8.22 (s, 1 H), 7.52 (d, J = 8.7 Hz, 2 H), 7.35 (d, J = 8.7 Hz, 2 H), 6.71 (s, 1 H), 4.47 (q, J = 7.1 Hz, 2 H), 1.44 (t, J = 7.1 Hz, 3 H); MS (ES) *m/z*: 355 (M + H^+).

5-{6-[*tert*-Butoxycarbonyl-(4-chloro-phenyl)-amino]-pyrazin-2-yl}-nicotinic Acid 22. Replacing **4** with **21** and following the same procedure as in the preparation of **5** gave **22** as a yellow solid: 94% yield; MS (ES) *m/z*: 427 (M + H^+).

[6-(5-*tert*-Butoxycarbonylamino-pyridin-3-yl)-pyrazin-2-yl]-(4-chloro-phenyl)-carbamic Acid *tert*-Butyl Ester 23. Replacing **5** with **22** and following the same procedure as in the preparation of **6** gave **23** as a foam: 55% yield: ^{1}H NMR (300 MHz, $CDCl_3$) δ 9.02 (s, 1 H), 8.78 (s, 1 H), 8.68 (d, J = 1.8 Hz, 1 H), 8.44 (d, J = 2.4 Hz, 2 H), 7.38 (d, J = 8.7 Hz, 2 H), 7.22 (d, J = 8.7 Hz, 2 H), 6.56 (brs, 1 H), 1.55 (s, 9 H), 1.48 (s, 9 H); MS (ES) *m/z*: 498 (M + H^+).

(4-Chloro-phenyl)-{6-[5-(3-pyridin-4-yl-propylamino)-pyridin-3-yl]-pyrazin-2-yl}-amine 24. Replacing **6** with **23** and following the same procedure as in the preparation of **20** gave **24** as a light yellow solid: 79% yield; ^{1}H NMR (300 MHz, CD_3OD) δ 8.39 (m, 4 H), 8.10 (s, 1 H), 7.98 (s, 1 H), 7.77 (m, 2 H), 7.61 (s, 1 H), 7.33 (d, J = 6.1 Hz, 2 H), 7.27 (dd, J = 6.9, 2.1 Hz, 2 H), 3.25 (t, J = 6.8 Hz, 2 H), 2.84 (t, J = 7.6 Hz, 2 H), 2.04 (m, 2 H); MS (ES) *m/z*: 417 (M + H^+); FAB-HRMS (M + H^+) calcd. for $C_{23}H_{23}ClN_6$ 417.1594, found 417.1588.

5-[6-(3,4-Dichloro-phenylamino)-pyrazin-2-yl]-nicotinic Acid Ethyl Ester 25. Replacing 3-chloroaniline with 3,4-dichloroaniline and following the same procedure as in the preparation of **4** gave **25** as a yellow solid: 24% yield; ^{1}H NMR (300 MHz, $CDCl_3$) δ 9.15 (d, J = 1.9 Hz, 1 H), 9.06 (d, J = 2.1 Hz, 1 H), 8.53 (s, 1 H), 8.45 (s, 1 H), 8.07 (m, 1 H), 7.50 (m, 1 H), 7.40 (m, 1 H), 7.21 (dd, J = 8.7, 1.5 Hz, 1 H), 4.45 (q, J = 7.1 Hz, 2 H), 1.44 (t, J = 7.1 Hz, 3 H); MS (ES) *m/z*: 389 (M + H^+).

5-{6-[*tert*-Butoxycarbonyl-(3,4-dichloro-phenyl)-amino]-pyrazin-2-yl}-nicotinic Acid 26. Replacing **4** with **25** and following the same procedure as in the preparation of **5** gave **26** as a yellow solid: 90% yield; MS (ES) *m/z*: 461 ($M + H^+$).

[6-(5-*tert*-Butoxycarbonylamino-pyridin-3-yl)-pyrazin-2-yl]-(3,4-dichloro-phenyl)-carbamic acid *tert*-butyl ester 27. Replacing **5** with **26** and following the same procedure as in the preparation of **6** gave **27** as a foam: 23% yield: ^{1}H NMR (300 MHz, $CDCl_3$) δ 8.99 (s, 1 H), 8.81 (s, 1 H), 8.69 (brs, 1 H), 8.45 (brs, 2 H), 7.49 (d, $J = 8.6$ Hz, 1 H), 7.40 (d, $J = 2.4$ Hz, 1 H), 7.16 (dd, $J = 8.6$ 2.4 Hz, 1 H), 6.59 (brs, 1 H), 1.54 (s, 9 H), 1.49 (s, 9 H); MS (ES) *m/z*: 532 ($M + H^+$).

(3,4-Dichloro-phenyl)-{6-[5-(3-pyridin-4-yl-propylamino)-pyridin-3-yl]-pyrazin-2-yl}-amine 28. Replacing **6** with **27** and following the same procedure as in the preparation of **20** gave **28** as a light yellow solid: 29% yield: ^{1}H NMR (300 MHz, DMSO-d_6) δ 9.97 (s, 1 H), 8.62 (s, 1 H), 8.46 (s, 2 H), 8.34 (d, $J = 2.1$ Hz, 1 H), 8.23 (s, 1 H), 8.08 (s, 1 H), 7.58 (m, 3 H), 7.31 (m, 2 H), 3.18 (m, 2 H), 2.76 (t, $J = 7.7$ Hz, 2 H), 1.93 (m, 2 H); MS (ES) *m/z*: 451 ($M+H^+$); FAB-HRMS ($M + H^+$) calcd. for $C_{23}H_{21}Cl_2N_6$ 451.1196, found 451.1205.

General Procedure for the Synthesis of 29 and 33. 5-(6-Benzylamino-pyrazin-2-yl)-nicotinic Acid Ethyl Ester 29. A mixture of **3** (320 mg, 1.22 mmol), benzylamine (144 mg, 1.34 mmol), $Pd_2(dba)_3$ (32 mg, 0.03 mmol), DPPF (54 mg, 0.096 mmol), and Cs_2CO_3 (795 mg, 2.44 mmol) in anhydrous dioxane (3.6 mL) was stirred at 110 °C for 39 h under nitrogen. The cooled reaction mixture was concentrated and purified by column chromatography to give 130 mg (28%) of **29** as a green oil: ^{1}H NMR (300 MHz, $CDCl_3$) δ 9.35 (d, $J = 2.2$ Hz, 1 H), 9.25 (d, $J = 2.0$ Hz, 1 H), 8.84 (t, $J = 2.0$ Hz, 1 H), 8.37 (s, 1 H), 7.94 (s, 1 H), 7.43−7.38 (m, 5 H), 5.13 (m, 1 H), 4.68 (d, $J = 5.7$ Hz, 2 H), 4.46 (q, $J = 7.2$ Hz, 2 H), 1.45 (t, $J = 7.2$ Hz, 3 H); FAB-HRMS ($M + H^+$) calcd. for $C_{19}H_{19}N_4O_2$ 335.1508, found 335.1515.

General Procedure for the Synthesis of 30 and 34. 5-[6-(Benzyl-*tert*-butoxycarbonyl-amino)-pyrazin-2-yl]-nicotinic Acid 30. A mixture of **29** (220 mg, 1.658 mmol), Boc_2O (431 mg, 1.98 mmol), and DMAP (30 mg, cat.) in dichloromethane (4.1 mL) was stirred at 20 °C for 4 days. The reaction mixture was concentrated, and the product was purified by column chromatography (EtOAc/hexane as solvent) to give 195 mg (68%) of **Boc-29** as a white solid: ^{1}H NMR (300 MHz, $CDCl_3$) δ 9.27 (dd, $J = 7.9$, 2.2 Hz, 2 H), 9.22 (s, 1 H), 8.78 (t, $J = 2.1$ Hz, 1 H), 8.74 (s, 1 H), 7.35−7.21 (m, 5 H), 5.30 (s, 2 H), 4.46 (q, $J = 7.1$ Hz, 2 H), 1.50 (s, 9 H), 1.43 (t, $J = 7.1$ Hz, 3 H); FAB-HRMS ($M + H^+$) calcd. for $C_{24}H_{27}N_4O_4$ 435.2032, found 435.2058.

A mixture of **Boc-29** (195 mg, 0.449 mmol) was dissolved in methanol (4.4 mL) and stirred for 10 min then cooled to 0 °C. $NaOH_{(aq)}$ (1 N, 0.94 mL) was added slowly, and the mixture was stirred at 0 °C for 10 min and then stirred at 20 °C for another 18 h. Glacial acetic acid (0.8 mL) was added to the reaction mixture at 0 °C slowly followed by the addition of water (3 mL). A solid was formed and was collected by filtration, washed with water (5×), and dried in a vacuum over overnight to give 399 mg (80%) of **30** as a white solid: ^{1}H NMR (300 MHz, CD_3OD) δ 9.29 (d, $J = 2.0$ Hz, 1 H), 9.17 (s, 1 H), 9.15 (d, $J = 1.6$ Hz, 1 H), 8.94 (t, $J = 2.1$ Hz, 1 H), 8.90 (s, 1 H), 7.42−7.19 (m, 5 H), 5.30 (s, 2 H), 1.50 (s, 9 H); MS (ES) *m/z*: 405 ($M - H^+$); Anal. ($C_{22}H_{22}N_4O_4 \cdot 0.4\ H_2O$) C, H, N.

General Procedure for the Synthesis of 31 and 35. Benzyl-[6-(5-*tert*-butoxycarboylamino-pyridin-3-yl)-pyrazin-2-yl]-carbamic acid *tert*-butyl Ester 31. A mixture of **30** (128 mg, 0.315 mmol), DPPA (104 mg, 0.38 mmol), triethylamine (64 mg, 0.68 mmol), and *t*-BuOH (1.33 mL) in toluene (0.95 mL) was stirred under nitrogen at 70 °C for 30 min and then at 100 °C for 19 h. The reaction mixture was concentrated under a vacuum. The product was purified by column chromatography (EtOAc/hexane as solvent) to give 89 mg (59%) of **31** as a white solid: ^{1}H NMR (300 MHz, $CDCl_3$) δ 9.13 (s, 1 H), 8.81 (d, $J = 1.8$ Hz, 1 H), 8.69 (s, 1 H), 8.55 (d, $J = 2.4$ Hz, 1 H), 8.38 (brs, 1 H), 7.35−7.21 (m, 5 H), 6.56 (brs, 1 H), 5.28 (s, 2 H), 1.55 (s, 9 H), 1.50 (s, 9 H); MS (ES) *m/z* 478 ($M + H^+$).

General Procedure for the Synthesis of 32 and 36. 3-[5-(6-Benzylamino-pyrazin-2-yl)-pyridin-3-yl-amino]-propan-1-ol 32. A mixture of **31** (83 mg, 0.174 mmol), (3-bromopropoxy)-*tert*-butyl-dimethylsilane (66 mg, 0.26 mmol), and Cs_2CO_3 (170 mg, 0.522 mmol) in DMF (2.1 mL) was stirred at 70 °C under nitrogen for 3 days. The reaction mixture was diluted with water, extracted with dichloromethane (3×), dried (Na_2SO_4), and concentrated. The product was purified by column chromatography (EtOAc/hexane as solvent) to give 54 mg of the silylated product as an orange oil. The silylated product was dissolved in TFA (0.6 mL) and stirred at 20 °C for 4 h before it was concentrated. An ammonium hydroxide solution was added to the residue until the pH was about 10−11, and a greenish solid was formed. The greenish solid was collected by filtration, washed with water, and dried under a vacuum. The greenish solid was recrystallized from CH_3OH/EtOAc to give 10 mg (17% two steps) of **32** as a light greenish solid: ^{1}H NMR (300 MHz, CD_3OD) δ 8.30 (s, 1 H), 8.15 (s, 1 H), 7.93 (brs, 1 H), 7.86 (s, 1 H), 7.54 (s, 1 H), 7.42−7.20 (m, 5 H), 4.64 (s, 2 H), 3.70 (t, $J = 6.1$ Hz, 2 H), 3.24 (t, $J = 6.6$ Hz, 2 H), 1.86 (m, 2 H); MS (ES) *m/z*: 336 ($M + H^+$); FAB-HRMS ($M + H^+$) calcd. for $C_{19}H_{22}N_5O$ 336.1824, found 336.1817.

5-[6-(3-Chloro-phenoxy)-pyrazin-2-yl]-nicotinic Acid Ethyl Ester 33. Replacing benzylamine with 3-chlorophenol and following the same procedure as in the preparation of **29** gave **33** as a solid: 27% yield; ^{1}H NMR (300 MHz, $CDCl_3$) δ 9.26 (brs, 2 H), 8.85 (s, 1 H), 8.73 (t, $J = 2.1$ Hz, 1 H), 8.46 (s, 1 H), 7.39 (t, $J = 8.4$ Hz, 1 H), 7.30−7.25 (m, 2 H), 7.16 (brd, $J = 8.2$ Hz, 1 H), 4.44 (q, $J = 7.1$ Hz, 2 H), 1.43 (t, $J = 7.1$ Hz, 3 H); Anal. ($C_{18}H_{14}ClN_3O_3$) C, H, N.

5-[6-(3-Chloro-phenoxy)-pyrazin-2-yl]-nicotinic Acid 34. Replacing **29** with **33** and following the same procedure as in the preparation of **30** gave **34** as a solid: 85% yield; ^{1}H NMR (300 MHz, CD_3OD) δ 9.23 (s, 1 H), 9.14 (s, 1 H), 9.00 (s, 1 H), 8.85 (t, $J = 2.1$ Hz, 1 H), 8.50 (s, 1 H), 7.47 (t, $J = 8.1$ Hz, 1 H), 7.39−7.23 (m, 3 H); MS (ES) *m/z*: 326 ($M - H^+$); Anal. ($C_{16}H_{10}ClN_3O_3$) C, H, N.

{5-[6-(3-Chloro-phenoxy)-pyrazin-2-yl]-pyridin-3-yl}-carbamic Acid *tert*-Butyl Ester 35. Replacing **30** with **34** and following the same procedure as in the preparation of **31** gave **35** as a solid: 40% yield; ^{1}H NMR (300 MHz, $CDCl_3$) δ 8.81 (s, 1 H), 8.78 (d, $J = 1.9$ Hz, 1 H), 8.51 (d, $J = 2.5$ Hz, 1 H), 8.44 (brs, 1 H), 8.40 (s, 1 H), 7.39 (t, $J = 8.2$ Hz, 1 H), 7.27−7.24 (m, 1 H), 7.17 (d, $J = 7.6$ Hz, 1 H), 6.57 (brs, 2 H), 1.54 (s, 9 H); FAB-HRMS ($M + H^+$) calcd. for $C_{20}H_{19}ClN_4O_3$ 399.1224, found 399.1241.

3-{5-[6-(3-Chloro-phenoxy)-pyrazin-2-yl]-pyridin-3-yl-amino}-propan-1-ol 36. Replacing **31** with **35** and following the same procedure as in the preparation of **32** gave **36** as a solid: 33% yield; ^{1}H NMR (300 MHz, CD_3OD) δ 8.87 (s, 1 H), 8.4 (s, 1 H), 8.28 (s, 1 H), 7.96 (d, $J = 2.7$ Hz, 1 H), 7.49−7.21 (m, 5 H), 3.67 (t, $J = 6.3$ Hz, 2 H), 3.20 (t, $J = 6.9$ Hz, 2 H), 1.82 (m, 2 H); MS (ES) *m/z*: 357 ($M + H^+$); FAB-HRMS ($M + H^+$) calcd. for $C_{18}H_{18}ClN_4O_2$ 357.1118, found 357.1120.

[6-(5-Amino-pyridin-3-yl)-pyrazin-2-yl]-(3-chloro-phenyl)-amine 37. Compound **6** (100 mg, 0.2 mmol) was dissolved in TFA (2 mL) and stirred at 20 °C for 2 h before it was concentrated. An ammonium hydroxide solution was added to the residue until the pH was about 10−11, water was added and a yellow solid was formed. The yellow solid was collected through filtration, washed with water, and dried under a vacuum to give 54 mg (91%) of **37** as a light yellow solid: MS (ES) *m/z*: 298 ($M + H^+$). Anal. ($C_{15}H_{12}ClN_5$) C, H, N.

General Procedure for the Synthesis of 38−41. 2-{5-[6-(3-Chloro-phenylamino)-pyrazin-2-yl]-pyridin-3-ylamino}-ethanol 38. A mixture of **6** (0.1 g, 0.2 mmol), (2-bromoethoxy)-*tert*-butyl-dimethylsilane (0.07 g, 0.3 mmol), and Cs_2CO_3 (0.197 g, 0.6 mmol) in DMF (4 mL) was stirred at 70 °C under nitrogen for 22 h. The reaction mixture was diluted with water, extracted with ether (3×), dried (Na_2SO_4), and concentrated. The product was purified by column chromatography (EtOAc/hexane as solvent) to give 0.05 g of the

silylated product as an oil. The silylated product was dissolved in TFA (1.5 mL) and stirred at 20 °C for 2 h before it was concentrated. An ammonium hydroxide solution was added to the residue until the pH was about 10−11, and a yellow solid was formed. The yellow solid was collected through filtration, washed with water, and dried under a vacuum to give 0.029 g (43%) of **38** as a light yellow solid: ^{1}H NMR (300 MHz, DMSO-d_6) δ 9.87 (s, 1 H), 8.59 (s, 1 H), 8.46 (s, 1 H), 8.22 (s, 1 H), 8.12 (m, 2 H), 7.61 (d, J = 8.2 Hz, 1 H), 7.52 (s, 1H), 7.37 (t, J = 8.1 Hz, 1 H), 7.03 (d, J = 7.8 Hz, 1 H), 6.10 (t, J = 5.3 Hz, 1 H), 4.79 (t, J = 5.3 Hz, 1 H), 3.63 (m, 2 H), 3.25 (m, 2 H); MS (ES) *m/z*: 342 (M+H$^+$); FAB-HRMS (M + H$^+$) calcd. for $C_{17}H_{16}ClN_5O$ 342.1122, found 342.1128.

4-{5-[6-(3-Chloro-phenylamino)-pyrazin-2-yl]-pyridin-3-ylamino}-butan-1-ol 39. Replacing (2-bromoethoxy)-*tert*-butyl-dimethylsilane with (4-bromobutoxy)-*tert*-butyl-dimethylsilane and following the same procedure as in the preparation of **38** gave **39** as a light yellow solid: 64% yield; ^{1}H NMR (300 MHz, DMSO-d_6) δ 9.88 (s, 1 H), 8.60 (s, 1 H), 8.45 (s, 1 H), 8.20 (m, 2 H), 8.08 (d, J = 2.5 Hz, 1 H), 7.56 (d, J = 8.2 Hz, 1 H), 7.48 (s, 1H), 7.36 (t, J = 8.0 Hz, 1 H), 7.03 (dd, J = 7.7, 1.4 Hz, 1 H), 6.12 (t, J = 5.2 Hz, 1 H), 4.45 (t, J = 5.1 Hz, 1 H), 3.44 (q, J = 6.1 Hz, 2 H), 3.15 (q, J = 6.2 Hz, 2 H), 1.59 (m, 4 H); MS (ES) *m/z*: 370 (M + H$^+$). Anal. ($C_{19}H_{20}ClN_5O$) C, H, N.

***N*-{5-[6-(3-Chloro-phenylamino)-pyrazin-2-yl]-pyridin-3-yl}-*N*′,*N*′-dimethyl-propane-1,3-diamine 40.** Replacing (2-bromoethoxy)-*tert*-butyl-dimethylsilane with 3-chloro-*N*,*N*-dimethylamine and following the same procedure as in the preparation of **38** gave **40** as a light yellow solid: 43% yield; ^{1}H NMR (300 MHz, CD_3OD) δ 8.42 (m, 2 H), 8.16 (t, J = 2.0 Hz, 1 H), 8.10 (s, 1 H), 8.00 (d, J = 2.6 Hz, 1 H), 7.63 (t, J = 2.0 Hz, 1 H), 7.48 (dd, J = 7.5, 1.2 Hz, 1 H), 7.28 (t, J = 8.0 Hz, 1 H), 6.98 (dd, J = 7.2, 1.1 Hz, 1 H), 3.27 (m, 2 H), 2.54 (brt, J = 7.5 Hz, 2 H), 2.30 (s, 6 H), 1.88 (m, 2 H); MS (ES) *m/z*: 383 (M + H$^+$). Anal. ($C_{20}H_{23}N_6OCl\cdot 0.9\ H_2O$) C, H, N.

***N*-{5-[6-(3-Chloro-phenylamino)-pyrazin-2-yl]-pyridin-3-yl}-*N*′,*N*′-dimethyl-ethane-1,2-diamine 41.** Replacing (2-bromoethoxy)-*tert*-butyl-dimethylsilane with 2-dimethylaminoethyl chloride hydrochloride and following the same procedure as in the preparation of **38** gave **41** as a light yellow solid: 41% yield; ^{1}H NMR (300 MHz, CD_3OD) δ 8.44 (m, 2 H), 8.13 (m, 2 H), 8.02 (d, J = 2.7 Hz, 1 H), 7.65 (m, 1 H), 7.52 (dd, J = 2.0, 0.9 Hz, 1 H), 7.29 (t, J = 8.0 Hz, 1 H), 7.00 (dd, J = 2.0, 0.9 Hz, 1 H), 3.36 (t, J = 6.5 Hz, 2 H), 2.64 (t, J = 6.5 Hz, 2 H), 2.32 (s, 6 H); MS (ES) *m/z*: 369 (M + H$^+$). Anal. ($C_{19}H_{21}ClN_6$) C, H, N.

General Procedure for the Synthesis of 42 and 43. 5-[6-(3-Chloro-phenylamino)-pyrazin-2-yl]-*N*-(2-(dimethylamino)-ethyl)-nicotinamide 42. A mixture compound **5** (0.05 g, 0.12 mmol), *N*,*N*-dimethylethylenediamine (0.01 g, 0.12 mmol), diisopropylethylamine (0.06 g, 0.47 mmol), and HATU (0.045 g, 0.12 mmol) in CH_2Cl_2 (2 mL) was stirred at 20 °C under N_2 for 2 days. Solvent was removed, and the product was purified by column chromatography (CH_2Cl_2/MeOH/acetic acid as solvent) to give 0.02 g of product. The above product was dissolved in TFA (1.0 mL) and stirred at 20 °C for 1 h before concentration. An ammonium hydroxide solution was added to the residue until the pH was about 10−11, and a yellow solid was formed. The yellow solid was collected through filtration, washed with water, and dried under a vacuum to give 0.005 g (11%) of **42** as a yellow solid: ^{1}H NMR (300 MHz, CD_3OD) δ 9.39 (s, 1 H), 9.06 (s, 1 H), 8.91 (s, 1 H), 8.59 (s, 1 H), 8.19 (s, 1 H), 8.07 (s, 1 H), 7.59 (d, J = 8.3 Hz, 1 H), 7.32 (t, J = 8.1 Hz, 1 H), 7.02 (d, J = 7.8 Hz, 1 H), 3.60 (t, J = 6.7 Hz, 2 H), 2.63 (t, J = 6.7 Hz, 2 H), 2.34 (s, 6 H); MS (ES) *m/z*: 397 (M + H$^+$); FAB-HRMS (M + H$^+$) calcd. for $C_{20}H_{21}ClN_6O$ 397.1543, found 397.1555.

5-[6-(3-Chloro-phenylamino)-pyrazin-2-yl]-*N*-(3-hydroxy-propyl)-nicotinamide 43. Replacing *N*,*N*-dimethylethylenediamine with 3-amino-1-propanol and following the same procedure as in the preparation of **42** gave **43** as a light yellow solid: 41% yield; ^{1}H NMR (300 MHz, CD_3OD) δ 9.38 (d, J = 2.0 Hz, 1 H), 9.02 (d, J = 2.0 Hz, 1 H), 8.86 (t, J = 2.0 Hz, 1 H), 8.58 (s, 1 H), 8.19 (s, 1 H), 8.06 (t, J = 2.0 Hz, 1 H), 7.59 (dd, J = 8.2, 1.3 Hz, 1 H), 7.31 (t, J = 8.0 Hz, 1 H), 7.02 (dd, J = 7.9, 1.1 Hz, 1 H), 3.68 (t, J = 6.2 Hz, 2 H), 3.55 (m, 2 H), 1.88 (t, J = 6.6 Hz, 2 H); MS (ES) *m/z*: 384 (M + H$^+$); FAB-HRMS (M + H$^+$) calcd. for $C_{19}H_{19}ClN_5O_2$ 384.1218, found 384.1227.

General Procedure for the Synthesis of 44−49. *N*-{5-[6-(3-Chloro-phenylamino)-pyrazin-2-yl]-pyridin-3-yl}-2-hydroxy-acetamide 44. A mixture of compound **6** (250 mg, 0.5 mmol) and 60% NaH (150 mg, 3.5 mmol) in THF (9 mL) was stirred under nitrogen at 20 °C for 0.5 h before acetoxyacetyl chloride (478 mg, 3.5 mmol) was added. The reaction was stirred at reflux for 18 h and cooled to room temperature. Water was added, and the reaction mixture was extracted with ethyl acetate. The organic layer was dried (Na_2SO_4), concentrated, and purified by column chromatography (EtOAc/acetone as solvent) to give 70 mg of the Boc-protected amide as an oil. The Boc-protected amide was stirred in dichloromethane (1.3 mL) and TFA (0.42 mL) at 20 °C for 60 h before concentrated. Ammonium hydroxide solution was added to the residue until the pH was about 10−11 and was then extracted with ethyl acetate. The ethyl acetate layer was dried (Na_2SO_4) and then concentrated under a vacuum and purified by column chromatography (EtOAc/acetone as solvent) to give 26 mg (13%) of **acetyl-44** as an off-white solid: ^{1}H NMR (300 MHz, CD_3OD) δ 8.91 (brs, 1 H), 8.75 (brs, 2 H), 8.42 (brs, 1 H), 8.10 (brs, 1 H), 7.83−7.56 (m, 2 H), 7.28 (m, 1 H), 6.96 (m, 1 H), 4.85 (s, 2 H), 2.21 (s, 3 H); MS (ES) *m/z*: 398 (M + 1$^+$).

A mixture of **acetyl-44** (26 mg, 0.065 mmol), K_2CO_3 (5.4 mg, 0.04 mmol), H_2O (0.1 mL), and methanol (3.4 mL) was heated at reflux for 1 min. Crystals were recovered by filtration and purified by recrystallization from methanol to give 5 mg (22%) of **44** as an off-white solid: ^{1}H NMR (300 MHz, CD_3OD) δ 10.10 (s, 1 H), 9.89 (s, 1 H), 8.98−8.88 (m, 3 H), 8.60 (s, 1 H), 8.26 (s, 1 H), 7.89−7.86 (m, 2 H), 7.40 (t, J = 8.2 Hz, 1 H), 7.04 (d, J = 7.2 Hz, 1 H), 5.81 (m, 1 H), 4.08 (d, J = 5.5 Hz, 2 H); FAB-HRMS (M + H$^+$) calcd. for $C_{17}H_{14}ClN_5O_2$ 356.0914, found 356.0927.

***N*-{5-[6-(3-Chloro-phenylamino)-pyrazin-2-yl]-pyridin-3-yl}-2-methoxy-acetamide 45.** Replacing acetoxyacetyl chloride with methoxyacetyl chloride and following the same procedure as in the preparation of **44** gave **45** as a yellow solid: 21% yield; ^{1}H NMR (300 MHz, CD_3OD) δ 8.98 (s, 1 H), 8.86 (brs, 2 H), 8.48 (s, 1 H), 8.15 (s, 1 H), 7.92 (s, 1 H), 7.72 (d, J = 8.1 Hz, 1 H), 7.32 (t, J = 8.0 Hz, 1 H), 6.99 (d, J = 7.8 Hz, 1 H), 4.11 (s, 2 H), 3.52 (s, 3 H); MS (ES) *m/z*: 370 (M + H$^+$).

***N*-{5-[6-(3-Chloro-phenylamino)-pyrazin-2-yl]-pyridin-3-yl}-3-methoxy-propionamide 46.** Replacing acetoxyacetyl chloride with 3-methoxypropanoyl chloride and following the same procedure as in the preparation of **44** gave **46** as an off-white solid: 26% yield; ^{1}H NMR (300 MHz, DMSO-d_6) δ 10.35 (s, 1 H), 9.89 (s, 1 H), 8.96 (s, 1 H), 8.81 (s, 1 H), 8.78 (s, 1 H), 8.60 (s, 1 H), 8.26 (s, 1 H), 7.88 (brs, 1 H), 7.84 (brs, 1 H), 7.40 (t, J = 8.1 Hz, 1 H), 7.04 (dd, J = 7.8, 1.1 Hz, 1 H), 3.66 (t, J = 6.1 Hz, 2 H), 3.26 (s, 3 H), 2.63 (t, J = 6.1 Hz, 2 H); Anal. ($C_{19}H_{18}ClN_5O_2\cdot 0.2\ H_2O$) C, H, N.

***N*-{5-[6-(3-Chloro-phenylamino)-pyrazin-2-yl]-pyridin-3-yl}-2-benzyloxy-acetamide 47.** Replacing acetoxyacetyl chloride with benzyloxyacetyl chloride and following the same procedure as in the preparation of **44** gave **47** as an off-white solid: 22% yield; ^{1}H NMR (300 MHz, -DMSO-d_6) δ 10.21 (s, 1 H), 9.89 (s, 1 H), 8.99 (d, J = 1.7 Hz, 1 H), 8.86 (brs, 1 H), 8.61 (s, 1 H), 8.27 (s, 1 H), 7.90 (brs, 1 H), 7.86 (d, J = 8.1 Hz, 1 H), 7.45−7.30 (m, 6 H), 7.03 (d, J = 9.4 Hz, 1 H), 4.67 (s, 2 H), 4.18 (s, 2 H); Anal. ($C_{24}H_{20}ClN_5O_2\cdot 0.2\ H_2O$) C, H, N.

***N*-{5-[6-(3-Chloro-phenylamino)-pyrazin-2-yl]-pyridin-3-yl}-2-phenoxy-acetamide 48.** Replacing acetoxyacetyl chloride with phenoxyacetyl chloride and following the same procedure as in the preparation of **44** gave **48** as an off-white solid: 23% yield; ^{1}H NMR (300 MHz, DMSO-d_6) δ 10.48 (s, 1 H), 9.89 (s, 1 H), 9.00 (d, J = 1.6 Hz, 1 H), 8.86 (brs, 2 H), 8.62 (s, 1 H), 8.26 (s, 1 H), 7.87 (s, 1 H), 7.84 (s, 1 H), 7.34 (t, J =

7.6 Hz, 3 H), 7.07−6.97 (m, 4 H), 4.79 (s, 2 H); FAB-HRMS (M + H$^+$) calcd. for $C_{23}H_{18}ClN_5O_2$ 432.1227, found 432.1238.

***N*-{5-[6-(3-Chloro-phenylamino)-pyrazin-2-yl]-pyridin-3-yl}-4-(dimethylamino)-benzamide 49.** Replacing acetoxyacetyl chloride with 4-dimethylaminobenzoyl chloride and following the same procedure as in the preparation of **44** gave **49** as an off-white solid: 49% yield; ^{1}H NMR (300 MHz, DMSO-d_6) δ 8.97 (m, 3 H), 8.63 (s, 1 H), 8.27 (s, 1 H), 7.96 (m, 3 H), 7.92 (s, 1 H), 7.84 (dd, J = 8.2, 1.3 Hz, 1 H), 7.41 (t, J = 8.0 Hz, 1 H), 7.04 (dd, J = 7.9, 1.4 Hz, 1 H), 6.79 (d, J = 9.0 Hz, 2 H), 3.02 (s, 6 H); MS (ES) *m/z*: 445 (M + H$^+$). Anal. ($C_{24}H_{21}N_6OCl$·1.15 H_2O) C, H, N.

General Procedure for the Synthesis of 50−62. *N*-(3-Chlorophenyl)-6-[5-[[3-(1-piperazinyl)propyl]amino]-3-pyridinyl]-2-pyrazinamine 50. 1-(3-Chloropropyl)-piperazine hydrochloride (1 g, 4.1 mmol) was dissolved in CH_2Cl_2 (20 mL) and treated with Boc_2O (1.78 g, 8.2 mmol), DMAP (cat.), and Et_3N (2.06 g, 20 mol). The reaction mixture was stirred at room temperature for 5 h and then refluxed overnight. The solvent was removed under a vacuum, and the product was purified by column chromatography (CH_2Cl_2/MeOH as solvent) to give 1 g (93%) of 4-(3-chloropropyl)-piperazine-1-carboxylic acid *tert*-butyl ester: ^{1}H NMR (300 MHz, $CDCl_3$) δ 3.60 (t, J = 6.5 Hz, 2 H), 3.42 (t, J = 5.0 Hz, 4 H), 2.48 (t, J = 6.9 Hz, 2 H), 2.38 (t, J = 5.0 Hz, 4 H), 1.94 (m, 2 H), 1.46 (s, 9 H); MS (ES) *m/z*: 263 (M + H$^+$).

A mixture of compound **6** (0.1 g, 0.2 mmol), 4-(3-chloropropyl)-piperazine-1-carboxylic acid *tert*-butyl ester (0.079 g, 0.3 mmol), and Cs_2CO_3 (0.197 g, 0.6 mmol) in DMF (4 mL) was stirred at 70 °C under nitrogen for 20 h. The reaction mixture was diluted with water, extracted with ether (3×), dried (Na_2SO_4), and concentrated. The product was purified by column chromatography (CH_2Cl_2/MeOH as solvent) to give 0.192 g of product as an oil. The oil was dissolved in TFA (2.0 mL) and stirred at 20 °C for 2 h before concentrated. Ammonium hydroxide solution was added to the residue until the pH was about 10−11, and a yellow solid was formed. The yellow solid was collected through filtration, washed with water, and dried under a vacuum to give 0.072 g (65%) of **50** as a yellow solid: ^{1}H NMR (300 MHz, CD_3OD) δ 8.43 (m, 2 H), 8.18 (d, J = 2.0 Hz, 1 H), 8.11 (s, 1 H), 8.00 (d, J = 2.5 Hz, 1 H), 7.65 (s, 1 H), 7.49 (brd, J = 8.0 Hz, 1 H), 7.29 (t, J = 8.0 Hz, 1 H), 6.99 (d, J = 7.0 Hz, 1 H), 3.30 (m, 2 H), 2.86 (m, 4 H), 2.51 (m, 6 H), 1.88 (m, 2 H); MS (ES) *m/z*: 424 (M + H$^+$). Anal. ($C_{22}H_{26}N_7Cl$·0.9 H_2O) C, H, N.

(3-Chlorophenyl)-(6-{5-[3-(4-methyl-piperazin-1-yl)-propylamino]-pyridin-3-yl}-pyrazin-2-yl)-amine 51. Replacing 4-(3-chloropropyl)-piperazine-1-carboxylic acid *tert*-butyl ester with 1-(3-chloropropyl)-4-methylpiperazine dihydrochloride and following the same procedure as in the preparation of **50** gave **51** as a solid: 61% yield; ^{1}H NMR (300 MHz, $CDCl_3$) δ 8.51 (s, 2 H), 8.16 (s, 1 H), 7.90 (t, J = 2.0 Hz, 1 H), 7.50 (t, J = 1.9 Hz, 1 H), 7.30 (m, 2 H), 7.06 (m, 1 H), 6.73 (s, 1 H), 5.42 (brs, 1 H), 3.33 (t, J = 5.3 Hz, 2 H), 2.55 (t, J = 6.3 Hz, 8 H), 2.30 (s, 3 H), 1.87 (m, 2 H), 1.66 (m, 2 H); FAB-HRMS (M + H$^+$) calcd. for $C_{23}H_{29}ClN_7$ 438.2173, found 438.2180.

***N*-[5-[6-[(3-Chlorophenyl)amino]pyrazinyl]-3-pyridinyl]-4-morpholinepropanamine 52.** Replacing 4-(3-chloropropyl)-piperazine-1-carboxylic acid *tert*-butyl ester with morpholinopropyl chloride and following the same procedure as in the preparation of **50** gave **52** as an off-white solid: 62% yield; ^{1}H NMR (300 MHz, CD_3OD) δ 8.43 (s, 1 H), 8.39 (d, J = 1.5 Hz, 1 H), 8.16 (d, J = 1.9 Hz, 1 H), 8.09 (s, 1 H), 7.99 (d, J = 2.3 Hz, 1 H), 7.64 (s, 1 H), 7.47 (d, J = 7.8. Hz, 1 H), 7.27 (t, J = 8.0 Hz, 1 H), 6.98 (d, J = 7.9 Hz, 1 H), 3.66 (m, 4 H), 3.28 (m, 2 H), 2.49 (m, 6 H), 1.85 (m, 2 H); MS (ES) *m/z*: 425 (M + H$^+$). Anal. ($C_{22}H_{25}N_6OCl$·0.55 H_2O) C, H, N.

(3-Chlorophenyl)-{6-[5-(3-piperidin-1-yl-propylamino)-pyridin-3-yl]-pyrazin-2-yl}-amine 53. Replacing 4-(3-chloropropyl)-piperazine-1-carboxylic acid *tert*-butyl ester with 1-(3-chloropropyl)piperidine and following the same procedure as in the preparation of **50** gave **53** as a light yellow solid: 83% yield; ^{1}H NMR (300 MHz, CD_3OD) δ 8.46 (s, 1 H), 8.42 (s, 1 H), 8.16 (s, 1 H), 8.11 (s, 1 H), 8.00 (s, 1 H), 7.65 (s, 1 H), 7.49 (d, J = 9.0 Hz, 1 H), 7.29 (t, J = 8.0 Hz, 1 H), 6.99 (d, J = 8.0 Hz, 1 H) 3.28 (m, 2 H), 2.57 (m, 6 H), 1.90 (m, 2 H), 1.63 (m, 4 H), 1.49 (d, J = 4.4 Hz, 2 H); MS (ES) *m/z*: 423 (M + H$^+$). Anal. ($C_{23}H_{27}N_6Cl$·0.7 H_2O) C, H, N.

***N*-(3-Chlorophenyl)-6-[5-[[(tetrahydro-2*H*-pyran-4-yl)-methyl]amino]-3-pyridinyl]-2-pyrazinamine 54.** Replacing 4-(3-chloropropyl)-piperazine-1-carboxylic acid *tert*-butyl ester with tetrahydropyranyl-4-methanesulfonate ester[36] and following the same procedure as in the preparation of **50** gave **54** as an off-white solid: 83% yield; ^{1}H NMR (300 MHz, $CDCl_3$) δ 8.53 (m, 2 H), 8.17 (s, 1 H), 8.10 (d, J = 2.6 Hz, 1 H), 7.90 (brs, 1 H), 7.53 (t, J = 2.2 Hz, 1 H), 7.29 (m, 2 H), 7.07 (m, 1 H), 6.69 (s, 1 H), 4.02 (dd, J = 11.3, 4.3 Hz, 2 H), 3.92 (brs, 1 H), 3.40 (td, J = 11.9, 1.8 Hz, 2 H), 3.17 (t, J = 6.0 Hz, 2 H), 1.90 (m, 1 H), 1.74 (brd, J = 12.8 Hz, 2 H), 1.42 (qd, J = 12.2, 4.2 Hz, 2 H); MS (ES) *m/z*: 396 (M + H$^+$). Anal. ($C_{21}H_{22}N_5ClO$·0.2 H_2O) C, H, N.

***N*-(3-Chlorophenyl)-6-[5-[[4-(4-pyridinyl)butyl]amino]-3-pyridinyl]-2-pyrazinamine 55.** Replacing 4-(3-chloropropyl)-piperazine-1-carboxylic acid *tert*-butyl ester with 4-(4-pyridinyl)butyl chloride[37] and following the same procedure as in the preparation of **50** gave **55** as a light yellow solid: 74% yield; ^{1}H NMR (300 MHz, $CDCl_3$) δ 8.52 (m, 4 H), 8.17 (s, 1 H), 8.09 (d, J = 2.3 Hz, 1 H), 7.92 (s, 1 H), 7.50 (s, 1 H), 7.28 (s, 1 H), 7.12 (d, J = 5.4 Hz, 2 H), 7.06 (m, 1 H), 6.83 (s, 1 H), 3.81 (brs, 1 H), 3.26 (q, J = 5.9 Hz, 2 H), 2.69 (t, J = 7.0 Hz, 2 H), 1.77 (m, 4 H); MS (ES) *m/z*: 431 (M + H$^+$). Anal. ($C_{24}H_{23}N_6Cl$·0.3 H_2O) C, H, N.

***N*-(3-Chlorophenyl)-6-[5-[[3-(3-pyridinyl)propyl]amino]-3-pyridinyl]-2-pyrazinamine 56.** Replacing 4-(3-chloropropyl)-piperazine-1-carboxylic acid *tert*-butyl ester with 3-(3-chloropropyl)pyridine[35] and following the same procedure as in the preparation of **50** gave **56** as a yellow solid: 78% yield; ^{1}H NMR (300 MHz, $CDCl_3$) δ 8.55 (m, 4 H), 8.24 (s, 1 H), 8.07 (s, 1 H), 7.81 (m, 2 H), 7.54 (m, 2 H), 7.27 (m, 2 H), 7.06 (d, J = 7.1 Hz, 1 H), 3.95 (m, 1 H), 3.28 (m, 2 H), 2.80 (t, J = 7.3 Hz, 2 H), 2.05 (m, 2 H); MS (ES) *m/z*: 417 (M + H$^+$). Anal. ($C_{23}H_{21}N_6Cl$·0.7 H_2O) C, H, N.

***N*-(3-Chlorophenyl)-6-[5-[[3-(1*H*-pyrazol-1-yl)propyl]-amino]-3-pyridinyl]-2-pyrazinamine 57.** 1-Bromo-3-chloropropane (11.3 g, 72 mmol) was added dropwise to a vigorously stirred ice-cooled mixture of pyrazole (5.0 g, 73 mmol), K_2CO_3 (10.0 g, 73 mmol), and acetone (95 mL). After 3 h, the cooling bath was removed, and the reaction mixture was stirred at 20 ° C for 5 days and then filtered. The filtrate was concentrated, and product was purified by column chromatography (using EtOAc/hexane as solvent) to give 3.3 g (31%) of 1-(3-chloro-propyl)-1*H*-pyrazole as a clear oil: ^{1}H NMR (300 MHz, $CDCl_3$) δ 7.52 (d, J = 1.5 Hz, 1 H), 7.42 (d, J = 2.1 Hz, 1 H), 6.24 (t, J = 2.0 Hz, 1 H), 4.32 (t, J = 6.4 Hz, 2 H), 3.45 (t, J = 6.0 Hz, 2 H), 2.32 (m, 2 H); MS (ES) *m/z*: 145 (M + H$^+$).

Replacing 4-(3-chloropropyl)-piperazine-1-carboxylic acid *tert*-butyl ester with 1-(3-chloro-propyl)-1*H*-pyrazole and following the same procedure as in the preparation of **50** gave **57** as an off-white solid: 90% yield; ^{1}H NMR (300 MHz, CD_3OD) δ 8.43 (s, 2 H), 8.10 (d, J = 7.9 Hz, 2 H), 7.98 (s, 1 H), 7.60 (m, 4 H), 7.27 (t, J = 8.0 Hz, 1 H), 6.98 (d, J = 7.9 Hz, 1 H), 6.26 (s, 1 H), 4.31 (t, J = 6.7 Hz, 2 H), 3.19 (t, J = 6.7 Hz, 2 H), 2.19 (m, 2 H); MS (ES) *m/z*: 406 (M + H$^+$). Anal. ($C_{21}H_{20}N_7Cl$·0.3 H_2O) C, H, N.

***N*-(3-Chlorophenyl)-6-[5-[[3-(1*H*-1,2,4-triazol-1-yl)propyl]amino]-3-pyridinyl]-2-pyrazinamine 58.** 1-Bromo-3-chloropropane (11.3 g, 72 mmol) was added dropwise under N_2 to a vigorously stirred ice-cooled mixture of 1,2,4-triazole (5.0 g, 72 mmol), K_2CO_3 (10.0 g, 73 mmol), and acetone (95 mL). After 3 h, the cooling bath was removed, and the reaction mixture stirred at 20 ° C for 5 days and then filtered. The filtrate was concentrated, and the product was purified by column chromatography (EtOAc/hexane as solvent) to give 7.1 g (68%) of 1-(3-chloro-propyl)-1*H*-[1,2,4]triazole as a clear oil: ^{1}H NMR (300 MHz, $CDCl_3$) δ 8.11 (s, 1 H), 7.96 (s, 1 H), 4.38

(t, J = 6.4 Hz, 2 H), 3.48 (t, J = 6.0 Hz, 2 H), 2.35 (m, 2 H); MS (ES) *m/z*: 146 ($M + H^+$).

Replacing 4-(3-chloropropyl)-piperazine-1-carboxylic acid *tert*-butyl ester with 1-(3-chloro-propyl)-1*H*-[1,2,4]triazole and following the same procedure as in the preparation of **50** gave **58** as a yellow solid: 86% yield; ^{1}H NMR (300 MHz, DMSO-d_6) δ 9.85 (s, 1 H), 8.59 (s, 1 H), 8.52 (s, 1 H), 8.47 (s, 1 H), 8.23 (s, 1 H), 8.12 (t, J = 1.9 Hz, 1 H), 8.08 (d, J = 2.6 Hz, 1 H), 7.96 (s, 1 H), 7.59 (d, J = 9.5 Hz, 1 H), 7.47 (s, 1 H), 7.33 (t, J = 8.1 Hz, 1 H), 7.02 (dd, J = 7.7, 1.6 Hz, 1 H), 6.23 (t, J = 5.5 Hz, 1 H), 4.33 (t, J = 6.9 Hz, 1 H), 3.15 (m, 2 H), 2.12 (m, 2 H); MS (ES) *m/z*: 407 ($M + H^+$). Anal. ($C_{20}H_{19}N_8Cl \cdot 0.4\ H_2O$) C, H, N.

(3-Chloro-phenyl)-{6-[5-(3-phenyl-propylamino)-pyridin-3-yl]-pyrazin-2-yl}-amine 59. Replacing 4-(3-chloropropyl)-piperazine-1-carboxylic acid *tert*-butyl ester with 1-chloro-3-phenylpropane and following the same procedure as in the preparation of **50** gave **59** as an off-white solid: 47% yield; ^{1}H NMR (300 MHz, DMSO-d_6) δ 9.85 (s, 1 H), 8.58 (s, 1 H), 8.45 (brs, 1 H), 8.22 (s, 1 H), 8.16 (s, 1 H), 8.09 (brs, 1 H), 7.56 (d, J = 8.0 Hz, 1 H), 7.47 (s, 1 H), 7.26 (m, 6 H), 7.02 (d, J = 7.9 Hz, 1 H), 6.19 (t, J = 5.5 Hz, 1 H), 3.17 (m, 2 H), 2.72 (t, J = 7.4 Hz, 2 H), 1.89 (m, 2 H); MS (ES) *m/z*: 416 ($M + H^+$). Anal. ($C_{24}H_{22}N_5Cl \cdot 0.1\ H_2O$) C, H, N.

(3-Chloro-phenyl)-{6-[5-(2-phenoxy-ethylamino)-pyridin-3-yl]-pyrazin-2-yl}-amine 60. Replacing 4-(3-chloropropyl)-piperazine-1-carboxylic acid *tert*-butyl ester with beta-bromophenetole and following the same procedure as in the preparation of **50** gave **60** as a yellow solid: 68% yield; ^{1}H NMR (300 MHz, DMSO-d_6) δ 9.85 (s, 1 H), 8.61 (s, 1 H), 8.49 (s, 1 H), 8.23 (s, 1 H), 8.14 (s, 1 H), 7.66 (m, 2 H), 7.31 (m, 3 H), 6.98 (m, 4 H), 6.39 (brs, 1 H), 4.19 (t, J = 5.2 Hz, 2 H), 3.59 (d, J = 5.3 Hz, 2 H); MS (ES) *m/z*: 418 ($M + H^+$). Anal. ($C_{23}H_{20}N_5ClO \cdot 0.2\ H_2O$) C, H, N.

4-{5-[6-(3-Chloro-phenylamino)-pyrazin-2-yl]-pyridin-3-ylamino}-butyric acid 61. 4-Chlorobutyryl chloride (14.1 g, 100 mmol) was added over 15 min to a cooled mixture of pyridine (7.91 g, 100 mmol) and *t*-BuOH (10.52 g, 125 mmol). The mixture was stirred at room temperature for 18 h. 10% Sulfuric acid (50 mL) was added, and the oil that was formed was separated. The aqueous layer was extracted with ether (30 mL), and the ether extract was combined with the oil. The combined organic layer was washed with water and dried (Na_2SO_4) to give 8.9 g (50%) of 4-chloro-butyric acid *tert*-butyl ester: ^{1}H NMR (300 MHz, $CDCl_3$) δ 3.58 (t, J = 6.4 Hz, 2 H), 2.40 (t, J = 7.2 Hz, 2 H), 2.04 (m, 2 H), 1.45 (s, 9 H); MS (ES) *m/z*: 179 ($M+H^+$).

Replacing 4-(3-chloropropyl)-piperazine-1-carboxylic acid *tert*-butyl ester with 4-chloro-butyric acid *tert*-butyl ester and following the same procedure as in the preparation of **50** gave **61** as a yellow solid: 27% yield; ^{1}H NMR (300 MHz, DMSO-d_6) δ 12.10 (brs, 1 H), 9.85 (s, 1 H), 8.60 (s, 1 H), 8.46 (s, 1 H), 8.22 (s, 1 H), 8.15 (s, 1 H), 8.08 (s, 1 H), 7.59 (d, J = 9.3 Hz, 1 H), 7.51 (s, 1 H), 7.36 (t, J = 8.1 Hz, 1 H), 7.03 (d, J = 7.8 Hz, 1 H), 6.19 (m, 1 H), 3.14 (q, J = 6.2 Hz, 2 H), 2.36 (t, J = 7.2 Hz, 2 H), 1.83 (m, 2 H); MS (ES) *m/z*: 384 ($M+H^+$); FAB-HRMS ($M + H^+$) calcd. for $C_{19}H_{19}ClN_5O_2$ 384.1227, found 384.1234.

4-{5-[6-(3-Chloro-phenylamino)-pyrazin-2-yl]-pyridin-3-ylamino}-1-piperidin-1-yl-butan-1-one 62. Replacing 4-(3-chloropropyl)-piperazine-1-carboxylic acid *tert*-butyl ester with 1-(4-chloro-1-oxobutyl)-piperidine and following the same procedure as in the preparation of **50** gave **62** as a yellow solid: 47% yield; ^{1}H NMR (300 MHz, $CDCl_3$) δ 8.51 (s, 2 H), 8.17 (s, 1 H), 8.09 (d, J = 2.7 Hz, 1 H), 7.87 (t, J = 2.0 Hz, 1 H), 7.54 (t, J = 2.2 Hz, 1 H), 7.31 (m, 2 H), 7.05 (dd, J = 3.4, 1.5 Hz, 1 H), 6.73 (s, 1 H), 4.45 (brs, 1 H), 3.56 (t, J = 5.9 Hz, 2 H), 3.38 (t, J = 5.4 Hz, 2 H), 3.32 (q, J = 6.7 Hz, 2 H), 2.48 (t, J = 6.7 Hz, 2 H), 2.05 (m, 2 H), 1.53 (m, 6 H); MS (ES) *m/z*: 451 ($M + H^+$); FAB-HRMS ($M + H^+$) calcd. for $C_{24}H_{27}ClN_6O$ 451.2017, found 451.2013.

(6-Amino-5-bromo-pyridin-3-yl)-carbamic Acid Benzyl Ester 64. Bromine (2.3 mL, 44.6 mmol) was added dropwise to a suspension of the 6-aminonicotinic acid **63** (5.08 g, 36.8 mmol) in water (20 mL) at 4 °C. After the completion of the addition, the cooling bath was removed, and the reaction mixture was stirred at room temperature for 4.5 h. Saturated $Na_2S_2O_5$ was added slowly to the stirred mixture. The solid was collected through filtration, washed with water, and dried under a vacuum overnight to give 9.30 g of 6-amino-5-bromonicotinic acid along with 3,5-dibromo-2-aminopyridine in an ~1:1 ratio as a greenish solid; MS (ES) *m/z*: 217 ($M + H^+$).

A mixture of the solid (4.00 g) containing 6-amino-5-bromonicotinic acid, DPPA (6.08 g, 22.1 mmol), triethylamine (2.80 g, 27.7 mmol), benzyl alcohol (3.8 mL, 36.8 mmol), and toluene (50 mL) was heated at 70 °C for 1 h and then at 100 °C for 1 h. After concentration of the sample, the reaction mixture was purified by flash chromatography (EtOAc/hexane as solvent) to give 1.31 g (26% in two steps) of compound **64** as a yellow solid: ^{1}H NMR (300 MHz, $CDCl_3$) δ 7.99 (brs, 1 H), 7.91(d, J = 2.3 Hz, 1 H), 7.39−7.34 (m, 5 H), 6.50 (brs, 1 H), 5.19 (s, 2 H), 4.79 (brs, 2 H); MS (ES) *m/z*: 324 ($M + H^+$). Anal. ($C_{13}H_{12}BrN_3O_2 \cdot 0.1\ H_2O$) C, H, N.

(6-Amino-5-bromo-pyridin-3-yl)-[3-(*tert*-butyl-diphenyl-silanyloxy)-propyl]-carbamic Acid Benzyl Ester 65. A mixture of compound **64** (685 mg, 2.13 mmol), (3-bromopropoxy)-*tert*-butyldiphenylsilane (965 mg, 2.56 mmol), and Cs_2CO_3 (1.04 g, 3.19 mmol) in dry DMF (20 mL) was heated at 70 °C for 3 h. The reaction mixture was concentrated and purified by column chromatography (EtOAc/hexane as solvent) to give 1.06 g (81%) of compound **65** as a yellow oil: ^{1}H NMR (300 MHz, $CDCl_3$) δ 7.88 (brs, 1 H), 7.61−7.58 (m, 5 H), 7.51 (brs, 1 H), 7.41−7.30 (m, 10 H), 5.12 (s, 2 H), 4.93 (s, 2 H), 3.74 (t, J = 7.4 Hz, 2 H), 3.65 (t, J = 6.0 Hz, 2 H), 1.82−1.73 (m, 2 H), 1.00 (s, 9 H); MS (ES) *m/z*: 620 ($M + H^+$).

(5-Bromo-6-fluoro-pyridin-3-yl)-[3-(*tert*-butyl-diphenyl-silanyloxy)-propyl]-carbamic Acid Benzyl Ester 66. Nitrosonium tetrafluoroborate (170 mg, 1.45 mmol) was added to the solution of compound **65** (680 mg, 1.10 mmol) in CH_2Cl_2 (20 mL) at 4 °C. After 1 h at 4 °C, more $NOBF_4$ (50 mg, 0.43 mmol) was added followed by the same amount of $NOBF_4$ (50 mg, 0.43 mmol) after another 1 h. After stirring of the sample for total 3 h at 4 °C, water was added. The aqueous solution was extracted with CH_2Cl_2. The combined organic layers were dried, concentrated, and flash chromatographed (EtOAc/hexane) to give 425 mg (62%) of compound **66** as a yellow oil: ^{1}H NMR (300 MHz, $CDCl_3$) δ 8.24 (d, J = 2.3 Hz, 1 H), 7.84 (brs, 1 H), 7.59−7.56 (m, 5 H), 7.45−7.27 (m, 10 H), 5.15 (s, 2 H), 3.83 (m, 2 H), 3.65 (t, J = 5.9 Hz, 2 H), 1.79 (m, 2 H), 1.00 (s, 9 H); MS (ES) *m/z*: 645 ($M + Na^+$). Anal. ($C_{32}H_{34}BrFN_2O_3Si \cdot 0.50\ H_2O$) C, H, N.

[6-(5-{Benzyloxycarbonyl-[3-(*tert*-butyl-diphenyl-silanyloxy)-propyl]-amino}-2-fluoro-pyridin-3-yl)-pyrazin-2-yl]-(3-chloro-phenyl)-carbamic Acid *tert*-Butyl Ester 69. A mixture of compound **66** (405 mg, 0.652 mmol), bis-(trimethyltin) (427 mg, 1.30 mmol), tetrakis(triphenylphosphine) palladium (76 mg, 0.066 mmol), LiCl (110 mg, 2.59 mmol), and 2,6-di-*tert*-butyl-4-methylphenol (6 mg, 0.03 mmol) in anhydrous 1,4-dioxane (10 mL) was refluxed at 100 °C for 4.5 h under nitrogen. After the solvent was removed under reduced pressure, the mixture was purified by flash chromatography (EtOAc/hexane as solvent) to give 375 mg (82%) of **67** as a clear oil: ^{1}H NMR (400 MHz, $CDCl_3$) δ 8.17 (s, 1 H), 7.59−7.57 (m, 5 H), 7.53 (s, 1 H), 7.44−7.27 (m, 10 H), 5.14 (s, 2 H), 3.84 (t, J = 7.5 Hz, 2 H), 3.66 (t, J = 5.8 Hz, 2 H), 1.82 (m, 2 H), 0.98 (s, 9 H), 0.38 (s, 9 H); MS (ES) *m/z*: 729 ($M + Na^+$).

A mixture of compound **67** (370 mg, 0.525 mmol), *N*-(*tert*-butoxycarbonyl)-*N*-(3-chlorophenyl)-2-amino-6-chloropyrazine **68** (200 mg, 0.588 mmol), dichlorobis-(triphenylphosphine)palladium (74 mg, 0.11 mmol), and LiCl (89 mg, 2.10 mmol) in anhydrous toluene (5 mL) was stirred at 100 °C for 19 h under nitrogen. After the solvent was removed under reduced pressure, the residue was purified by flash chromatography (EtOAc/hexane as solvent) to give 140 mg (32%) of **69** as a yellow solid: ^{1}H NMR (400 MHz, $CDCl_3$) δ 9.15 (s, 1 H), 8.94 (d, J = 1.6 Hz, 1 H), 8.06 (s, 1 H), 7.89 (brs, 1 H),

7.59−7.52 (m, 5 H), 7.41−7.20 (m, 13 H), 7.06−7.04 (m, 1 H), 5.13 (s, 2 H), 3.78 (t, J = 7.3 Hz, 2 H), 3.62 (t, J = 5.9 Hz, 2 H), 1.76−1.70 (m, 2 H), 1.48 (s, 9 H), 0.95 (s, 9 H); MS (ES) *m/z*: 868 (M + Na^+).

3-{5-[6-(3-Chloro-phenylamino)-pyrazin-2-yl]-6-fluoro-pyridin-3-ylamino}-propan-1-ol 70. The mixture of compound **69** (100 mg, 0.118 mmol), 10% Pd/C (100 mg), EtOH (9 mL), and EtOAc (3 mL) was hydrogenated under 22 psi for 46 h at room temperature. After the solvents were removed under reduced pressure, the residue was purified by flash chromatography (ethyl acetate/hexane as solvent) to give 55 mg (65%) of the **des-Cbz-69** compound as a yellow oil. Anal. ($C_{39}H_{43}ClFN_5O_3Si$·0.30 H_2O) C, H, N.

A solution of the **des-Cbz-69** (68 mg, 0.096 mmol), TFA (1 mL), and CH_3SO_3H (3 drops) was stirred at room temperature for 5 h and then concentrated. A saturated NH_4OH solution was added to the residue until the mixture was made basic followed by the addition of water. The precipitated solid was collected through filtration, washed with water, and dried under a vacuum. The product was purified by flash chromatography on silica gel (using EtOAc/MeOH as the solvent) to provide 30 mg (84%) of **70** as a yellow solid: ^{1}H NMR (300 MHz, DMSO-d_6) δ 9.90 (s, 1 H), 8.42 (s, 1 H), 8.25 (s, 1 H), 8.05 (s, 1 H), 7.64 (s, 1 H), 7.62 (s, 2 H), 7.36 (t, J = 8.1 Hz, 1 H), 7.03 (d, J = 7.8 Hz, 1 H), 6.02 (brs, 1 H), 4.52 (brs, 1 H), 3.54 (t, J = 5.9 Hz, 2 H), 3.17 (m, 2 H), 1.76 (m, 2 H); MS (ES) *m/z*: 374 (M + H^+); FAB-HRMS (M + H^+) calcd. for $C_{18}H_{17}ClFN_5O$ 374.1184, found 374.1179.

5-Bromo-6-chloro-nicotinic Acid 72. Bromine (4.2 mL, 81.4 mmol) was added dropwise to the suspension of 6-hydroxynicotinic acid **71** (8.00 g, 57.6 mmol) in water (30 mL) at 4 °C. After the addition was completed, the cooling bath was removed, and the reaction mixture was stirred at room temperature for 4 h. Saturated $Na_2S_2O_5$ was added slowly to the stirred mixture until the brown mixture became white. The solid was collected through filtration, washed with water, and dried under a vacuum overnight to give 12.17 g (97%) of 6-hydroxy-5-bromonicotinic acid as an off-white solid: ^{1}H NMR (300 MHz, DMSO-d_6) δ 12.95 (brs, 1 H), 12.55 (brs, 1 H), 8.16 (s, 1 H), 8.04 (s, 1 H).

Quinoline (1.0 mL, 8.47 mmol) was slowly added to the solution of $POCl_3$ (2.0 mL, 21.5 mmol), followed by 6-hydroxy-5-bromonicotinic acid (3.92 g, 18.0 mmol) at room temperature. After the sample was heated at 120 °C for 2 h, the reaction was quenched by addition of water dropwise at ∼100 °C. After the mixture was cooled at 4 °C for a few hours, the solid was collected through filtration, washed with water, and dried under a vacuum overnight to give 3.68 g (87%) of **72** as an off-white solid: ^{1}H NMR (300 MHz, DMSO-d_6) δ 8.86 (s, 1 H), 8.55 (s, 1 H); MS (ES) *m/z*: 236 (M − H^+).

(5-Bromo-6-chloro-pyridin-3-yl)-carbamic Acid *tert*-Butyl Ester 73. A mixture of **72** (2.00 g, 8.46 mmol), DPPA (3.49 g, 12.7 mmol), triethylamine (2.56 g, 25.3 mmol), *t*-BuOH (18 mL), and toluene (20 mL) was heated at 65 °C for 3 h and then at 100 °C for 1.5 h. After the solvent was removed under reduced pressure, the reaction mixture was purified by flash chromatography (EtOAc/hexane as solvent) to give 3.04 g of **73** as an off-white solid: ^{1}H NMR (300 MHz, $CDCl_3$) δ 8.36 (s, 1 H), 8.19 (d, J = 2.3 Hz, 1 H), 7.01 (brs, 1 H), 1.52 (s, 9 H); MS (ES) *m/z*: 309 (M+H^+). Anal. ($C_{10}H_{12}BrClN_2O_2$) C, H, N.

(5-Bromo-6-chloro-pyridin-3-yl)-(3-hydroxy-propyl)-carbamic Acid *tert*-Butyl Ester 74. A mixture of compound **73** (710 mg, 2.31 mmol), 3-bromo-1-propanol (400 mg, 2.88 mmol), and Cs_2CO_3 (1.13 g, 3.47 mmol) in dry CH_3CN (10 mL) was heated at 65 °C for 17 h. The reaction mixture was concentrated and purified by column chromatography (EtOAc/hexane as solvent) to give 255 mg (30%) of **74** as a clear oil: ^{1}H NMR (300 MHz, $CDCl_3$) δ 8.22 (d, J = 2.4 Hz, 1 H), 7.84 (d, J = 2.3 Hz, 1 H), 3.80 (t, J = 6.5 Hz, 2 H), 3.67 (m, 2 H), 1.74 (m, 2 H), 1.44 (s, 9 H); MS (ES) *m/z*: 389 (M + Na^+).

(6-Chloro-5-trimethylstannanyl-pyridin-3-yl)-(3-hydroxy-propyl)-carbamic Acid *tert*-Butyl Ester 75. A mixture of **74** (145 mg, 0.396 mmol), bis(trimethyltin) (260 mg, 0.794 mmol), tetrakis(triphenylphosphine) palladium (46 mg, 0.040 mmol), LiCl (68 mg, 1.6 mmol), and 2,6-di-*tert*-butyl-4-methylphenol (4 mg, 0.02 mmol) in anhydrous 1,4-dioxane (5 mL) was refluxed at 100 °C for 3 h under nitrogen. After the solvent was removed under reduced pressure, the residue was purified by flash chromatography (CH_2Cl_2/EtOAc as solvent) to give 149 mg (84%) of **75** as a clear oil: ^{1}H NMR (300 MHz, $CDCl_3$) δ 8.13 (d, J = 2.9 Hz, 1 H), 7.50 (d, J = 2.9 Hz, 1 H), 3.79 (t, J = 6.3 Hz, 2 H), 3.67 (m, 2 H), 1.71 (m, 2 H), 1.42 (s, 9 H), 0.42 (s, 9 H); MS (ES) *m/z*: 451 (M + H^+).

3-{6-Chloro-5-[6-(3-chloro-phenylamino)-pyrazin-2-yl]-pyridin-3-ylamino}-propan-1-ol 76. A mixture of **75** (145 mg, 0.323 mmol), *N*-(*tert*-butoxycarbonyl)-*N*-(3-chlorophenyl)-2-amino-6-chloropyrazine **68** (120 mg, 0.353 mmol), dichlorobis(triphenylphosphine)palladium (23 mg, 0.033 mmol), and LiCl (55 mg, 1.3 mmol) in anhydrous toluene (4 mL) was stirred at 110 °C for 32 h under nitrogen. After the solvent was removed under reduced pressure, the residue was purified by flash chromatography (EtOAc/hexane as solvent) to give 28 mg (15%) of the coupling compound as a yellow solid. A solution of the yellow solid (28 mg, 0.047 mmol), TFA (1 mL), and CH_2Cl_2 (1 mL) was stirred at room temperature for 1.5 h and then concentrated. A saturated NH_4OH solution was added to the residue until the mixture became basic, followed by the addition of water. The precipitated solid was collected through filtration, washed with water, and dried under a vacuum. The product was purified by flash chromatography on silica gel (EtOAc/CH_2Cl_2 as solvent) to provide 13 mg (70%) of **76** as a yellow solid: ^{1}H NMR (300 MHz, DMSO-d_6) δ 9.89 (s, 1 H), 8.26 (s, 2 H), 8.07 (s, 1 H), 7.86 (d, J = 2.9 Hz, 1 H), 7.57 (d, J = 8.3 Hz, 1 H), 7.32 (t, J = 8.1 Hz, 1 H), 7.20 (d, J = 2.9 Hz, 1 H), 6.99 (d, J = 6.0 Hz, 1 H), 6.26 (t, J = 5.2 Hz, 1 H), 4.50 (brs, 1 H), 3.50 (m, 2 H), 3.15 (m, 2 H), 1.72 (m, 2 H); MS (ES) *m/z*: 390 (M + H^+); FAB-HRMS (M + H^+) calcd. for $C_{18}H_{17}Cl_2N_5O$ 390.0888, found 390.0901.

(6-Amino-5-trimethylstannanyl-pyridin-3-yl)-[3-(*tert*-butyl-diphenyl-silanyloxy)-propyl]-carbamic Acid Benzyl Ester 77. A mixture of compound **65** (1.25 g, 2.02 mmol), bis(trimethyltin) (1.00 g, 3.05 mmol), tetrakis(triphenylphosphine) palladium (240 mg, 0.208 mmol), LiCl (260 mg, 6.13 mmol), and 2,6-di-*tert*-butyl-4-methylphenol (20 mg, 0.091 mmol) in anhydrous 1,4-dioxane (25 mL) was refluxed at 100 °C for 3 h under nitrogen. After the solvent was removed under reduced pressure, the residue was purified by flash chromatography (EtOAc/hexane as solvent) to give 1.05 g (74%) of **77** as a yellow oil: ^{1}H NMR (300 MHz, $CDCl_3$) δ 7.86 (brs, 1 H), 7.61−7.58 (m, 5 H), 7.43−7.28 (m, 11 H), 5.11 (brs, 2 H), 4.40 (s, 2 H), 3.75 (t, J = 7.6 Hz, 2 H), 3.66 (t, J = 6.0 Hz, 2 H), 1.85−1.76 (m, 2 H), 0.99 (s, 9 H), 0.34 (s, 9 H); MS (ES) *m/z*: 704 (M + H^+).

[6-(2-Amino-5-{benzyloxycarbonyl-[3-(*tert*-butyl-diphenyl-silanyloxy)-propyl]-amino}-pyridin-3-yl)-pyrazin-2-yl]-(3-chloro-phenyl)-carbamic Acid *tert*-Butyl Ester 78. A mixture of compound **77** (1.05 g, 1.50 mmol), *N*-(*tert*-butoxycarbonyl)-*N*-(3-chlorophenyl)-2-amino-6-chloropyrazine **68** (510 mg, 1.50 mmol), dichlorobis(triphenylphosphine)palladium (105 mg, 0.150 mmol), and LiCl (190 mg, 4.48 mmol) in anhydrous toluene (30 mL) was stirred at 100 °C for 2.5 h under nitrogen. After the solvent was removed under reduced pressure, the residue was purified by flash chromatography (EtOAc/hexane as solvent) to give 830 mg (66%) of **78** as a yellow oil: ^{1}H NMR (300 MHz, $CDCl_3$) δ 9.00 (s, 1 H), 8.52 (brs, 1 H), 7.93 (s, 1 H), 7.66 (brs, 1 H), 7.59−7.55 (m, 5 H), 7.41−7.27 (m, 13 H), 7.14 (m, 1 H), 5.89 (s, 2 H), 5.11 (brs, 2 H), 3.77 (t, J = 7.4 Hz, 2 H), 3.65 (t, J = 5.9 Hz, 2 H), 1.84−1.75 (m, 2 H), 1.48 (s, 9 H), 0.97 (s, 9 H); MS (ES) *m/z*: 843 (M + H^+). Anal. ($C_{47}H_{51}ClN_6O_5Si$.1.70 H_2O) C, H, N.

3-{6-Amino-5-[6-(3-chloro-phenylamino)-pyrazin-2-yl]-pyridin-3-ylamino}-propan-1-ol 79. A solution of compound **78** (70 mg, 0.083 mmol), CF_3SO_3H (0.4 mL), and CH_2Cl_2 (1 mL) was stirred at room temperature for 1.5 h and then concentrated. A saturated NH_4OH solution was added to the residue at 4 °C until the mixture was made basic followed by the addition of water. The aqueous solution was discarded. The gummy material left in the reaction flask was washed with

water, dried under a vacuum, and purified by flash chromatography (CH_2Cl_2/MeOH as solvent) to provide 37 mg (76%) of **79** as a dark yellow oil: ^{1}H NMR (300 MHz, MeOH-d_4) δ 8.31 (s, 1 H), 8.07 (s, 1 H), 7.71 (s, 1 H), 7.61 (d, J = 2.5 Hz, 1 H), 7.47 (m, 2 H), 7.29 (t, J = 8.0 Hz, 1 H), 7.01 (d, J = 6.6 Hz, 1 H), 3.71 (t, J = 6.2 Hz, 2 H), 3.19 (t, J = 6.9 Hz, 2 H), 1.85 (m, 2 H); MS (ES) m/z: 371 ($M + H^+$); FAB-HRMS ($M + H^+$) calcd. for $C_{18}H_{19}ClN_6O$ 371.1387, found 371.1391.

Biology. Kinase Activity Assays. A kinase reaction mixture was prepared in 50 mM Tris-Cl (pH 8), 10 mM $MgCl_2$, 0.1 mM Na_3VO_4, 1 mM DTT, 1% DMSO, 0.25 μM biotinylated peptide substrate, 0.2−0.8 μCi per well ^{33}P-γ-ATP [2000−3000 Ci/mmol] and 5 μM ATP in the presence or absence of test compound and incubated at 30 °C for 1 h in a streptavidin coated FlashPlate (Perkin-Elmer, Boston, MA). Biotinylated peptide substrates were described as follows:[38] VEGF-R2 (biotin-KHKKLAEGSAYEEV-amide), calmodulin kinase 2 (biotin-KKALRRQETVDAL-amide), casein kinase-1 (biotin-KRRRALS(phospho)VASLPGL-amide), casein kinase-2 (biotin-RREEETEEE-amide), CDK1 (biotin-KTPKKAKKPKTPKK-AKKL-amide), CDK4 (GST-retinoblastoma protein construct), EGFR (biotin-DRVYIHPF-amide), FGFR-2 (biotin-poly(GT) 4:1), GSK-3 (biotin-KRREILSRRP(phospho)SYR-amide), insulin-R kinase (biotin-TRDIYETDYYRK-amide), MAPK (biotin-APRTPGGRR-amide), PDGF-R (biotin-KHKKLAEGSAY-EEV-amide), PKA (biotin-GRTGRRNSI-amide), PKCβ2 (biotin-RFARKGSLRQKNV-amide), and PKCγ (biotin-RFARKG-SLRQKNV-amide). Reaction conditions and components varied slightly depending on the protein kinase being assayed. The reaction was terminated by washing with PBS containing 100 mM EDTA, and plates were counted in a scintillation counter. Inhibition of the enzymatic activity due to the compound was measured by observing a reduced amount of ^{33}P-γ-ATP incorporated into the immobilized peptide relative to untreated controls. Linear regression analysis of the percent of inhibition by the test compound was used to calculate IC_{50} values (GraphPad Prism 3, GraphPad Software, San Diego, CA).

Cell Culture. HUVEC and HASMC cells were obtained from Cascade Biologicals (Portland, OR) and maintained in Media 200 containing low serum growth supplement (Cascade Biologicals). All other cells were obtained from the American Type Culture Collection (Manassas, VA). HeLa, A375, and HCT-116 cells were cultured in minimal essential medium (MEM) with 0.1 mM nonessential amino acids and 1 mM sodium pyruvate supplemented with 2 mM L-glutamine and 10% FCS (Hyclone, Logan, UT). MRC5 were cultured in Eagle's MEM and A375 were cultured in Dulbecco's modified Eagle's medium with 4 mM L-glutamine and 1.5 g/L sodium bicarbonate supplemented with 10% FCS. Cells were maintained at 37 °C plus 5% CO_2 as exponentially growing monolayers.

VEGF-Stimulated HUVEC Proliferation. To evaluate inhibition of VEGF-stimulated proliferation, HUVEC cells were detached with trypsin and seeded into 96-well plates in F-12K medium (Invitrogen, Carlsbad, CA) containing 0.2% heat-inactivated fetal bovine serum. Cells were stimulated with 2 ng/well VEGF (R&D Systems) in the presence or absence of test compounds. BrdU was added 24 h after the addition of VEGF and incubated with cells for an additional 20−24 h. BrdU incorporation was quantified using cell proliferation ELISA, BrdU reagents (Roche Biochemicals, Indianapolis, IN).

Cell Proliferation Assay. The ability of the test compound to inhibit the proliferation of cell growth was determined by measuring ^{14}C-thymidine incorporation into primary cells or cell lines derived from carcinomas originating from several tissues. Briefly, cells were trypsinized and seeded into 96-well CytoStar scintillating microplates (Amersham, Piscataway, NJ) in complete medium in a volume of 100 μL. Cells were incubated for 24 h at 37 °C in an atmosphere containing 5% CO_2. The test compound was added, and cells were incubated for 24 more hours. Methyl ^{14}C-thymidine (Perkin-Elmer, Boston, MA) was diluted in complete medium, and 0.2 μCi was added to each well of the CytoStar plate in a volume of 20 μL. The plate was incubated for 24 additional hours in the presence of test compound. Plates were washed twice with 200 μL of PBS, and ^{14}C-thymidine incorporation was quantified on a Packard Top Count. IC_{50} values reported as >10 indicate inhibition did not reach 50% of control at the highest dose tested.

In Vivo Antitumor Model. The VEGFR-2 inhibitors have been submitted to Piedmont Research Center (PRC) for evaluation against the A375 human melanoma xenograft growing in nude mice. Female *nu*/*nu* mice, 8 weeks of age were fed ad libitum water and an autoclaved standard rodent diet consisting of 5% fat, 6% fiber, 8% ash, 10% moisture, and 3% minerals. Female nude mice were implanted subcutaneously with 1 mm^3 A375 melanoma fragments in the flank. Tumors were monitored twice weekly and then daily as the neoplasms reached the desired size range (about 75 mg). Animals were pair-matched on day 1 when their tumors were in the 62−126 mg range, and the group mean tumor sizes were 66−71 mg. Estimated tumor weight was calculated using the formula: tumor weight (mg) = $(w^2l)/2$, where w = width and l = length in millimeters of an A375 melanoma. The VEGFR-2 inhibitors were provided preformulated for i.p. administration in a vehicle consisting of 1.5% Pluronic F108. Control groups included a no treatment tumor growth control group (10 mice) and a vehicle control group (6 mice). Each of the VEGFR-2 inhibitors were administered as i.p. at 75 or 10 mg/kg on a qd × 30 schedule. DTIC was given i.p. at 90 mg/kg on a qd × 5 schedule. All therapies were initiated on day 1, and the experiment was terminated on day 60. The tumor growth delay method was used in this study. Each animal was euthanized when its A375 neoplasm reached a size of 2.0 g. Mean day of survival (MDS) values were calculated for all groups. The MDS values calculated for each group based on the calculated day of death of each mouse as given by the formula:

$$\text{time to endpoint (calculated)} = \text{time to exceed endpoint (observed)} - \frac{\text{Wt}_2 - \text{endpoint weight}}{(\text{Wt}_2 - \text{Wt}_1)/(\text{D}_2 - \text{D}_1)}$$

where time to exceed endpoint (observed) = number of days it takes for each tumor to grow past the endpoint (cutoff) size. This is the day the animal is euthanized as a cancer death. D_2 = day the animal is euthanized. D_1 = last day of caliper measurement before tumor reaches the endpoint. Wt_2 = tumor weight on D_2. Wt_1 = tumor weight on D_1. Endpoint weight = predetermined "cutoff" tumor size for the model being used.

Animals were weighted twice weekly during the study. Mice were examined frequently for clinical signs of any adverse, drug-related side effects. Acceptable toxicity for cancer drugs in mice is defined by the NCI as no mean group weight loss of over 20% during the test and not more than one toxic death among 10 treated animals. The unpaired t-test and Mann−Whitney U test were used to determine the statistical significance of any difference in survival times between a treatment group and the control group. All statistical analyses were conducted at a p level of 0.05 (two-tailed).

Computational Details. As previously described,[25] a model of VEGFR-2 in complex with **7** was developed, based on the X-ray structure of VEGFR-2[41] (PDB code: 1VR2). This model was then used as the target structure for docking all the compounds reported here. The standard precision (SP) mode of the docking program Glide[39] was used to identify favorable binding poses. Glide allows the conformation and the position of a ligand be flexibly explored inside the binding pocket while holding the protein rigid during docking. The top 10 docking poses with the best Emodel scores[40] were saved for each compound, and the ones that led to the best QSAR model were eventually selected as the predicted binding poses. The selection procedure was conducted as follows. The top 1 pose with the best Emodel score was initially picked for each compound. After further geometry optimization, each complex structure was scored as in-place by GlideScore.[40] The value of each GlideScore component was extracted and used to build a QSAR model by linear regression, and its leave-one-out cross-

validated q^2 value was calculated. Then, the compound with the worst cross-validation prediction was reexamined, and another one from its top 10 docking poses was selected. After repeating the above steps, another QSAR model was developed, and its q^2 value was calculated. If the new q^2 value became better than the old one, the new docking pose was kept to replace the old one for that particular compound; otherwise, the new pose selection was rejected, and another pose would be tried. This procedure was repeated until a QSAR model with a satisfying q^2 value was obtained.

Each ligand−receptor complex structure was optimized by energy minimization in the aqueous solution, treated by the implicit GB/SA water model.[42] To prevent the unrealistic movement that may be caused by using implicit water model, harmonic position constraints of 100 and 10 kj/(Å^2 mol) were applied to the residues that were more than 12 Å away or within 6 to 12 Å from any ligand atom, respectively, while the ligand and the residues that are less than 6 Å away from the ligand were treated without position constraints.

All the molecular mechanism calculations were done using the program MacroModel[43] with OPLS_AA force field.[44] The Polak-Ribiere conjugate gradient method was used for energy minimization and the derivative convergence criterion was set at 0.05 kj/(Å mol). The QSAR analysis was conducted using the program MOE.[45]

Acknowledgment. We thank High Output Synthesis team help to scale-up some of the compounds for biological evaluation.

Supporting Information Available: Elemental analyses data are available free of charge via the Internet at http://pubs.acs.org.

References

(1) Risau, W. Mechanism of angiogenesis. *Nature* **1997**, *386*, 671−674.
(2) Ribatti, D.; Vacca, A.; Nico, B.; Roncali, L.; Dammacco, F. Postnatal angiogenesis. *Mech. Dev.* **2001**, *100*, 157−163.
(3) (a) Folkman, J. Anti-angiogenesis: new concept for therapy of solid tumors. *Ann. Surg*. **1972**, *175*, 409−416. (b) Folkman, J. Tumor angiogenesis: therapeutic implications. *N. Engl. J. Med.* **1971**, *285*, 1182−1186.
(4) Spranger, J.; Pfeiffer, A. F. New concepts in pathogenesis and treatment of diabetic retinopathy. *Exp. Clin. Endocrinol. Diabetes* **2001**, *109* (Suppl. 2) S438−S450.
(5) Walsh, D. A.; Haywood, L. Angiogenesis: a therapeutic target in arthritis. *Curr. Opin. Invest. Drugs* **2001**, *2*, 1054−1063.
(6) McLaren, J.; Prentice, A.; Charnock-Jones, D. S.; Millican, S. A.; Muller, K. H.; Sharkey, A. M.; Smith, S. K. Vascular endothelial growth factor is produced by peritoneal fluid macrophages in endometriosis and is regulated by ovarian steroids. *J. Clin. Invest*. **1996**, *98*, 482−489.
(7) Detmar, M. The role of VEGF and thrombospondin in skin angiogenesis. *Dermatol. Sci.* **2000**, *24*, S78−S84.
(8) Folkman, J. What is the evidence that tumors are angiogenesis dependment? *J. Natl. Cancer Inst.* **1990**, *82*, 4−6.
(9) Liotta, L. A.; Steeg, P. S.; Stetler-Stevenson, W. G. Cancer metastasis and angiogenesis: an imbalance of positive and negative regulation. *Cell* **1991**, 64, 327−336.
(10) (a) Nugent, M. A.; Iozzo, R. V. Fibroblast growth factor-2. *Int. J. Biochem. Cell. Biol*. **2000**, *32*, 115−120. (b) Carmeliet, P. Mechanisms of angiogenesis and arteriogenesis. *Nat. Med*. **2000**, *6*, 389−395. (c) Davis, S.; Yancopoulos, G. D. The angiopoietins: yin and yang in angiogenesis. *Curr. Top. Microbiol. Immunol.* **1999**, *237*, 173−185. (d) Lindahl, P.; Bostrom, H.; Karlsson, L.; Hellstrom, M.; Kalen, M.; Betsholtz, C. Role of platelet-derived growth factors in angiogenesis and alveogenesis. *Curr. Top. Pathol*. **1999**, *93*, 27−33.
(11) (a) Cross, M. J.; Claesson-Welsh, L. FGF and VEGF function in angiogenesis: signaling pathways, biological responses, and therapeutic inhibition. *Trends Pharm. Sci*. **2001**, *22*, 201−207. (b) McMahon, G. VEGF receptor signaling in tumor angiogenesis. *Oncologist* **2000**, *5* (Suppl. 1), 3−10. (c) Ferrara, N.; Davis-Smyth, T. The biology of vascular endothelial growth factor. *Endocrinol. Rev*. **1997**, *18*, 4−25.
(12) De Vries, C.; Escobedo, J. A.; Ueno, H.; Houck, K.; Ferrara, N.; Williams, L. T. The fms-like tyrosine kinase, a receptor for vascular endothelial growth factor. *Science* **1992**, *255*, 989−991.
(13) Shalaby, F.; Rossant, J.; Yamaguchl, T. P.; Gertsenstein, M.; Wu, X.-F.; Breltman, M. L.; Schuh, A. C. Failure of blood-island formation and vasculogenesis in Flk-1-deficient mice. *Nature* **1995**, *376*, 62−66.
(14) Ferrara, N.; Gerber, H.-P.; LeCouter, J. The biology of VEGF and its receptors. *Nat. Med.* **2003**, *9*, 669−676.
(15) Kerbel, R. S. A cancer therapy resistant to resistance. *Nature* **1997**, *390*, 335−336.
(16) Yang, J. C.; Haworth, L.; Sherry, R. M.; Hwu, P.; Schwartzentruber, D. J.; Topalian, S. L.; Steinberg, S. M.; Chen, H. X.; Rosenberg, S. A. A randomized trial of bevacizumab (anti-VEGF antibody) in metastatic renal cancer. *N. Eng. J. Med*. **2003**, *349*, 427−434.
(17) Prewett, M.; Huber, J.; Li, Y.; Santiago, A.; O'Connor, W.; King, K.; Overholser, J.; Hooper, A.; Pytowski, B.; Witte, L.; Bohlen, P.; Hicklin, D. J. Antivascular endothelial growth factor receptor (fetal liver kinase 1) monoclonal antibody inhibits tumor angiogenesis. *Cancer Res*. **1999**, *59*, 5209−5218.
(18) Holash, J.; Davis, S.; Papadopoulos, N.; Croll, S. D.; Ho, L.; Russell, M.; Boland, P.; Leidich, R.; Hylton, D.; Burova, E.; Ioffe, E.; Huang, T.; Radziejewski, C.; Baily, K.; Fandl, J. P.; Daly, T.; Wiegand, S. J.; Yancopoulos, G. D.; Rudge, J. S. VEGF-Trap: a VEGF blocker with potent antitumor effects. *Proc. Natl. Acad. Sci., U.S.A.* **2002**, *99*, 11393−11398.
(19) (a) Drevs, J.; Müller-Driver, R.; Wittig, C.; Fuxius, S.; Esser, N.; Hugenschmidt, H.; Konerding, M. A.; Allegrini, P. R.; Wood, J.; Hennig, J.; Unger, C.; Marmé, D. PTK787/ZK222584, a specific vascular endothelial growth factor-receptor tyrosine kinase inhibitor, effects the anatomy of the tumor vascular bed and the functional vascular properties as detected by dynamic enhanced magnetic resonance imaging. *Cancer Res*. **2002**, *62*, 4015−4022. (b) Bold, G.; Altman, K.-H.; Frei, J.; Lang, M.; Manley, P. W.; Traxler, P.; Wietfeld, B.; Brüggen, J.; Buchdunger, E.; Cozens, R.; Ferrari, S.; Furet, P.; Hofmann, F.; Martiny-Baron, G.; Mestan, J.; Rösel, J.; Sills, M.; Stover, D.; Acemoglu, F.; Boss, E.; Emmenegger, R.; Lässer, L.; Masso, E.; Roth, R.; Schlachter, C.; Vetterli, W.; Wyss, D.; Wood, J. M. New anilinophthalazines as potent and orally well absorbed inhibitors of the VEGF receptor tyrosine kinase useful as antagonists of tumor-driven angiogenesis. *J. Med. Chem*. **2000**, *43*, 2310−2323.
(20) (a) Mendel, D. B.; Laird, A. D.; Xin, X.; Louie, S. G.; Christensen, J. G.; Li, G.; Schreck, R. E.; Abrams, T. J.; Ngai, T. J.; Lee, L. B.; Murray, L. J.; Carver, J.; Chan, E.; Moss, K. G.; Haznedar, J. O.; Sukbuntherng, J.; Blake, R. A.; Sun, L.; Tang, C.; Miller, T.; Shirazian, S.; McMahon, G.; Cherrington, J. M. In vivo antitumor activity of SU11248, a novel tyrosine kinase inhibitor targeting vascular endothelial growth factor and platelet-derived growth factor receptors: determination of a pharmacokinetic/pharmacodynamic relationship. *Clin. Cancer Res*. **2003**, *9*(1), 327−337. (b) Sepp-Lorenzino, L.; Thomas, K. A. *Expert Opin. Invest. Drugs* **2002**, *11*, 1−18.
(21) Abdollahi, A.; Lipson, K. E.; Han, X.; Krempien, R.; Trinh, T.; Weber, K. J.; Hahnfeldt, P.; Hlatky, L.; Debus, J.; Howlett, A. R.; Huber, P. E. SU5416 and SU6668 attenuate the angiogenic effects of radiation-induced tumor cell growth factor production and amplify the direct anti-endothelial action of radiation in vitro. *Cancer Res*. **2003**, *63*, 3755−3763.
(22) (a) Ciardiello, F.; Caputo, R.; Damiano, V.; Caputo, R.; Troiani, T.; Vitagliano, D.; Carlomagno, F.; Veneziani, B. M.; Fontanini, G.; Bianco, A. R.; Tortora, G. Antitumor effects of ZD6474, a small molecule vascular endothelial growth factor receptor tyrosine kinase inhibitor, with additional activity against epidermal growth factor receptor tyrosine kinase. *Clin. Cancer Res.* **2003**, *9*, 1546−1556. (b) Hennequin, L. F.; Stokes, E. S.; Thomas, A. P.; Johnstone, C.; Plé, P. A.; Ogilvie, D. J.; Dukes, M.; Wedge, S. R.; Kendrew, J.; Curwen, J. O. Novel 4-anilinoquinazolines with C-7 basic side chains: design and structure activity relationship of a series of potent, orally active, VEGF receptor tyrosine kinase inhibitors. *J. Med. Chem*. **2002**, *45*, 1300−1312.
(23) Kabbinavar, F.; Hurwitz, H. I.; Fehrenbacher, L.; Meropol, N. J.; Novotny, W. F.; Lieberman, G.; Griffing, S.; Bergsland, E. Phase II, randomized trial comparing bevacizumab plus fluorouracil (FU)/leucovorin (LV) with FU/LV alone in patients with metastatic colorectal cancer. *J. Clin. Oncol*. **2003**, *21*, 60−65.
(24) (a) Gingrich, D. E.; Reddy, D. R.; Iqbal, M. A.; Singh, J.; Almone, L. D.; Angeles, T. S.; Albom, M.; Yang, S.; Ator, M. A.; Meyer, S. L.; Robinson, C.; Ruggeri, B. A.; Dionne, C. A.; Vaught, J. L.; Mallamo, J. P.; Hudkins, R. L. A new class of potent vascular endothelial growth factor receptor tyrosine kinase inhibitors: structure−activity relationships for a series of 9-alkoxymethyl-12-(3-hydroxypropyl)indeno[2, 1-*a*]pyrrolo[3, 4-*c*]carbazole-5-ones and the identification of CEP-5214 and its dimethylglycine ester prodrug clinical candidate CEP-7055. *J. Med. Chem*. **2003**, *46*, 5375−5388. (b) Boyer, S. J. Small molecule inhibitors of KDR (VEGFR-2) kinase: an overview of structure activity relationships. *Curr. Top. Med. Chem*. **2002**, *2*, 973−1000. (c) Connell, R. D. Patent focus on cancer chemotherapeutics V. Angiogenesis agents: September 2001-August 2002. *Expert Opin. Ther. Pat.* **2002**, *12*, 1763−1782.

(25) Kuo, G.-H.; Wang, A.; Emanuel, S.; DeAngelis, A.; Zhang, R.; Connolly, P. J.; Murray, W. V.; Gruninger, R. H.; Sechler, J.; Fuentes-Pesquera, A.; Johnson, D.; Middleton, S. A.; Jolliffe, L.; Chen, X. Synthesis and Discovery of Pyrazine-Pyridine Biheteroaryl as a Novel Series of Potent Vascular Endothelial Growth Factor Receptor-2 Inhibitors *J. Med. Chem*. **2005**, *48*, 1886−1900.

(26) Farina, V.; Krishnan, B. Large rate accelerations in the Stille reaction with tri-2-furylphosphine and triphenylarsine as palladium ligands: mechanistic and synthetic implications. *J. Am. Chem. Soc.* **1991**, *113*, 9585−9595.

(27) (a) Wolfe, J. P.; Buchwald, S. L. Palladium-catalyzed amination of aryl triflates. *J. Org. Chem*. **1997**, *62*, 1264−1267. (b) Aranyos, A.; Old, D. W.; Kiyomori, A.; Wolfe, J. P.; Sadighi, J. P.; Buchwald, S. L. Novel electron-rich bulky phosphine ligands facilitate the palladium-catalyzed preparation of diaryl ethers. *J. Am. Chem. Soc*. **1999**, *121*, 4369−4378.

(28) Reisch, J.; Dziemba, P.; Mura, M. L.; Rao, A. R. R. Natural product chemistry. Part 159 [1]. Two methods for the synthesis of 4-azaacronycine as a potential antitumor agent. *J. Heterocycl. Chem*. **1993**, *30*, 981−983.

(29) Fujita, M.; Oka, H.; Ogura, K. Palladium(0)/LiCl promoted cross-coupling reaction of (4-pyridyl)stannanes and aromatic bromides: easy access to poly(4-pyridyl)-substituted aromatics. *Tetrahedron Lett.* **1995**, *36*, 5247−5250.

(30) Brown, A. D.; Dickinson, R. P.; Wythes, M. J. Indole derivatives as 5-HT-like agonists. WO 93/21178.

(31) Mann, G.; Hartwig, J. F.; Driver, M. S.; Fernández-Rivas, C. Palladium-catalyzed C-N(sp^2) bond formation: *N*-arylation of aromatic and unsaturated nitrogen and the reductive elimination chemistry of palladium azolyl and methyleneamido complexes. *J. Am. Chem. Soc.* **1998**, *120*, 827−828.

(32) Brogi, E.; Wu, T.; Namiki, A.; Isner, J. M. Indirect angiogenic cytokines upregulate VEGF and bFGF gene expression in vascular smooth muscle cells, whereas hypoxia upregulates VEGF expression only. *Circulation* **1994**, *90*, 649−652.

(33) Kilic, T.; Alberta, J. A.; Zdunek, P. R.; Acar, M.; Iannarelli, P.; O'Reilly, T.; Buchdunger, E.; Black, P. M.; Stiles, C. D. Intracranial inhibition of platelet-derived growth factor-mediated glioblastoma cell growth by an orally active kinase inhibitor of the 2-phenylaminopyrimidine class. *Cancer Res*. **2000**, *60*, 5143−5150.

(34) (a) Compounds **56**, **57**, and **58** were not evaluated further because of the strong inhibition of CYP450 enzymes were observed in human liver microsomal studies. Compounds **39** and **41** demonstrated low oral bioavailability (F < 10%) and therefore were administered through i.p. route for the in vivo studies. (b) The A375 melanoma is considered to be a good target for VEGFR-2 inhibitors because it has good vascularization, which supports its rapid growth kinetics. (c) Serrone, L.; Zeuli, M.; Sega, F. M.; Cognetti, F. Dacarbazine-based chemotherapy for metastatic melanoma: thirty year experience overview. *J. Exp. Clin. Cancer Res*. **2000**, *19*, 21−34.

(35) Eisch, J. J.; Gopal, H.; Russo, D. A. Preparation and aluminum chloride induced rearrangement of cyclopropylpyridines. *J. Org. Chem*. **1974**, *39*, 3110−3114.

(36) Caldwell, W. S.; Bencherif, M.; Dull, G. M.; Crooks, P. A.; Lippiello, P. M.; Bhatti, B. S.; Deo, N. M.; Ravard, A. 3-Pyridyl-1-azabicycloalkane derivatives for prevention and treatment of CNS disorders. WO9900385, CAN 130:105302.

(37) Chung, J. Y. L.; Zhao, D.; Hughes, D. L.; Grabowski, E. J. J. A practical synthesis of fibrinogen receptor antagonist MK-383. Selective functionalization of (S)-tyrosine. *Tetrahedron* **1993**, *49*, 5767−5776.

(38) Emanuel, S.; Gruninger, R. H.; Fuentes-Pesquera, A.; Connolly, P. J.; Seamon, J. A.; Hazel, S.; Tominovich, R.; Hollister, B.; Napier, C.; Reuman, M.; Bignan, G.; Tuman, R.; Johnson, D.; Moffatt, D.; Batchelor, M.; Foley, A.; O'Connell, J.; Allen, R.; Perry, M.; Jolliffe, L.; Middleton, S. A. A VEGF-R2 kinase inhibitor potentiates the activity of the conventional chemotherapeutic agents paclitaxel and doxorubicin in tumor xenograft models. *Mol. Pharm*. **2004**, *66*, 635−647.

(39) *Glide*; Schrodinger: Portland, OR.

(40) Friesner, R. A.; Banks, J. L.; Murphy, R. B.; Halgren, T. A.; Klicic, J. J.; Mainz, D. T.; Repasky, M. P.; Knoll, E. H.; Shelley, M.; Perry, J. K.; Shaw, D. E.; Francis, P.; Shenkin, P. S. Glide. A new approach for rapid, accurate docking and scoring. 1. method and assessment of docking accuracy. *J. Med. Chem*. **2004**, *47*, 1739−1749.

(41) McTigue, M. A.; Wickersham, J. A.; Pinko, C.; Showalter, R. E.; Parast, C. V.; Tempczyk-Russell, A.; Gehring, M. R.; Mroczkowski, B.; Kan, C.-C.; Villafranca, J. E.; Appelt, K. Crystal structure of the kinase domain of human vascular endothelial growth factor receptor 2: a key enzyme in angiogenesis. *Structure* **1999**, *7*, 319−330.

(42) Still, W. C.; Tempczyk, A.; Hawley, R. C.; Hendrickson, T. Semianalytical treatment of salvation for molecular mechanics and dynamics. *J. Am. Chem. Soc*. **1990**, *112*, 6127−6129.

(43) *MacroModel*; Schrodinger: Portland, OR.

(44) Jorgensen, W. L.; Maxwell, D. S.; Tirado-Rives, J. Development and testing of the OPLS all-atom force field on conformational energetics and properties of organic liquids. *J. Am. Chem. Soc*. **1996**, *118*, 11225−11235.

(45) *MOE*; Chemical Computing Group, Inc.: Montreal, Quebec, Canada.

JM058205B